NOAA TR ERL 358-AL 11

NOAA Technical Report ERL 358-AL 11

U.S. DEPARTMENT OF COMMERCE
NATIONAL OCEANIC AND ATMOSPHERIC ADMINISTRATION
Environmental Research Laboratories

A VHF Transmitter and System Synchronizer for Use in a Portable Doppler Radar System

PAUL E. JOHNSTON
WARNER L. ECKLUND
RAYMOND A. GREENWALD

BOULDER, COLO.
FEBRUARY 1976

U.S. DEPARTMENT OF COMMERCE
Elliot L. Richardson, Secretary
NATIONAL OCEANIC AND ATMOSPHERIC ADMINISTRATION
Robert M. White, Administrator
ENVIRONMENTAL RESEARCH LABORATORIES
Wilmot N. Hess, Director

NOAA TECHNICAL REPORT ERL 358-AL 11

A VHF Transmitter and System Synchronizer for Use in a Portable Doppler Radar System

PAUL E. JOHNSTON
WARNER L. ECKLUND
RAYMOND A. GREENWALD

BOULDER, COLO.
February 1976

For sale by the Superintendent of Documents, U. S. Government Printing Office, Washington, D. C. 20402

Table of Contents

A VHF TRANSMITTER AND SYSTEM SYNCHRONIZER FOR USE IN A PORTABLE DOPPLER RADAR SYSTEM

Paul E. Johnston, Warner L. Ecklund, and Raymond A. Greenwald

ABSTRACT

A portable 50 MHz transmitter capable of 15 kW peak rf power output at up to 5 percent duty cycles is described. The transmitter and a system synchronizer, also described, are combined with a frequency-coherent receiver, an on-line minicomputer processor with oscillographic display, and a novel collinear antenna to provide a highly portable VHF Doppler radar system. The system, complete with 5-degree azimuthal beamwidth antenna, weighs about 250 kg, and can be installed in remote locations in a few days. It has been used successfully in studies of equatorial and auroral ionospheric irregularities during the past several years.

1. INTRODUCTION

The scatter radar group of the Aeronomy Laboratory, NOAA, has made extensive use of 50 MHz radars to investigate ionospheric irregularities in both the equatorial and auroral regions. Much of this research, performed at established field sites, has used permanently installed transmitters and antenna arrays. However, to make the technique more flexible we have developed a completely portable system that can be set up in a few days so that VHF Doppler radar observations can be made at any desired location. This is an important consideration in making eclipse observations, in supporting rocket launches, and in performing multiple-station experiments. The complete portable system, weighing about 250 kg, consists of the units shown in the block diagram of Figure 1. The frequency-coherent receiver and analog tape recorder have been described in a report by Balsley(1971), the digital computer and computer display have been described by Greenwald(1972), and the narrow beam portable antenna has been described by Balsley and Ecklund(1972). The remaining major components of a complete portable Doppler radar system are the transmitter and system synchronizer. This report describes these two devices in detail. The diode switch used to control the transmitter excitation is also described since it is an important system element.

2. TRANSMITTER

2.1 General considerations

In addition to portability, cost, and ease of maintenance at remote locations, a major consideration in the transmitter design was the need for high peak rf power at low duty cycles (1 to 5 percent). We chose the 4-1000 as the final stage tube, since it can be operated at very high plate voltages in class C operation. At 10 kilovolts of plate voltage, the 4-1000 easily provides 15 kW of peak rf power. The plate can be operated at 15 kV to obtain over 20 kW of peak rf power, but with less stability and reliability of operation. The frequency-coherent rf pulse from the diode switch/preamplifier combination shown in Figure 1 provides about 20 mW of peak rf power to the transmitter input. Thus, we needed 60 dB of gain in the transmitter to obtain approximately 20 kW of peak rf power out. This was achieved by using three class-C stages of nearly identical design, with the input and output of each stage externally accessible to facilitate stage-by-stage testing.

Another general consideration involved the power supply design. Two power supplies were designed to provide the different voltages needed to operate the three amplifier stages. One supply gives the positive voltages needed for the plate and screen of the first two stages and the screen of the final stage amplifier. The other power supply provides the negative voltages needed for the grid bias of the three stages.

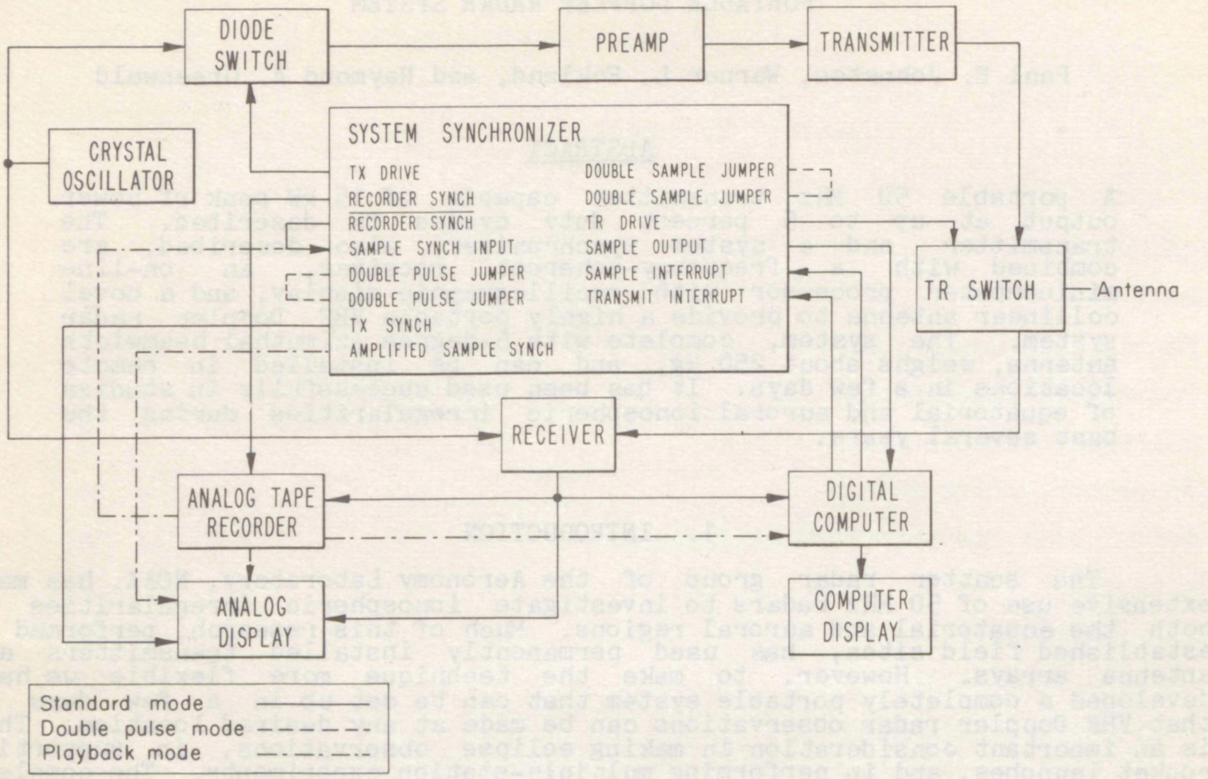

Figure 1. Block diagram of VHF Doppler radar system. All connections needed to operate the system are shown.

Finally, our use of the same antenna for transmission and reception has required the use of a transmit/receive switch with good receiver isolation and low insertion loss. In this design the TR switch (described in section 2.4) was built into the transmitter unit.

2.2 Mechanical construction

Figures 2 and 3 show the front and back of the complete three stage transmitter. The transmitter dimensions are approximately 60 cm x 45 cm x 30 cm. The transmitter enclosure is constructed of irridited aluminum for good electrical contact between plates. Pop rivets are used to fasten the plates together. The top and bottom plates are attached with sheet metal screws for access to the interior. Two cooling fans are mounted externally as shown in Figures 2 and 3.

The front panel switches numbered 1, 2, and 3 in Figure 2 control the fans, the filament and bias power supply, and the plate-screen power supply. Above the switches are the tuning controls for the second-stage amplifier (grid control (No. 4), plate control (No. 5), and output control (No. 6)). The three knobs to the right are the tuning controls for the final amplifier stage (grid control (No. 7), plate control (No. 8), and output control (No. 9)).

The rear view of the transmitter (Fig. 3) shows the a.c. power jack, rf inputs, and outputs for the three amplifier stages (first-stage input, No. 10; first-stage output, No.11; second-stage input, No. 12; second-stage output, No. 13; third-stage input, No.14; third-stage output, No.15). The connections between stages are made externally when the transmitter is in operation. At the left edge of the transmitter in Figure 3 are the TR switch drive input (No. 16) and the receiver input connection (No. 17). The final-stage plate voltage jack (No. 18) is shown with its plastic cover on. The final-stage plate voltage is provided by a commercially available 10 kV, 150 mA power supply.

The transmitter is divided into four compartments. Figure 4 shows the two top compartments with the top plate removed. The first-stage is in a separate aluminum box (see Fig. 5) mounted in the smaller top compartment. Grid, plate, and output tuning for this stage are accessible on the top of the first stage box (see both Figs. 4 and 5). The second-stage tube and its associated plate and output circuitry are also located in the smaller compartment (lower lefthand corner of Fig. 4 and greater detail in Fig. 6). The final-stage tube, plate, and output circuitry are located in the large compartment. The aluminum cover along the top of the large compartment shown in Figure 4 contains the one-microfarad, 15-kV capacitor that filters the final stage plate supply. The TR switch box is located under the large, air-variable, output tuning capacitor situated along the right edge of the larger compartment shown in Figure 4. The TR switch box (with cover removed) is shown in detail in Figure 7.

Figure 8 shows a view of the transmitter with bottom plate removed. The smaller compartment on the left contains the grid bias supply and the bottom of the second-stage tube socket which is shown in more detail in Figure 9. The large compartment in Figure 8 contains the plate-screen power supply and the final-stage tube socket. The ten square units on the power supply board (upper right corner) are heat-sinks for the high-voltage zener diode regulator string. The large fan input is located so that the air flows across these heat-sinks and into the socket of the final tube. In addition, a 1-inch diameter hole in the lower partition between the large and small compartments provides a small cooling air flow through the second-stage tube.

2.3 Electronic construction

Figure 10 shows a block diagram of the transmitter. Notice that the plate-screen power supply provides voltages for all three stages. The bias supply also is used for all stages.

The primary power schematic is shown in Figure 11. Note that filament power and grid-bias voltage cannot be applied to the tubes until the fans are running, and that plate and screen voltages cannot be applied unless the fans, filaments, and grid bias are activated.

Figures 12 and 13 are the schematics of the plate-screen and bias power supplies. Both circuits are full wave voltage doublers with zener diode regulation. Ripple in these power supplies is approximately 0.01 percent. Regulation is less than 10 percent, with peak current capacity being provided by filter capacitors on the output of each power supply. All zener diodes have rf bypass capacitors to reduce rf noise.

Figure 12 is the schematic of the plate-screen power supply. The zener diode regulator string operates with a quiescent current of 35 mA.

Figure 13 is a schematic of the grid bias power supply. The transformer (T1) used in this supply was chosen because it is interchangeable with T3 and T4 used in the plate-screen supply.

Figure 14 shows the first-stage schematic. The 6CL6 amplifier has an inductively-linked input that provides an rf pulse to the grid which is d.c. biased for class C operation. The gain of this stage is approximately 20 dB (20 mW of input rf power provides 2 watts peak rf power output).

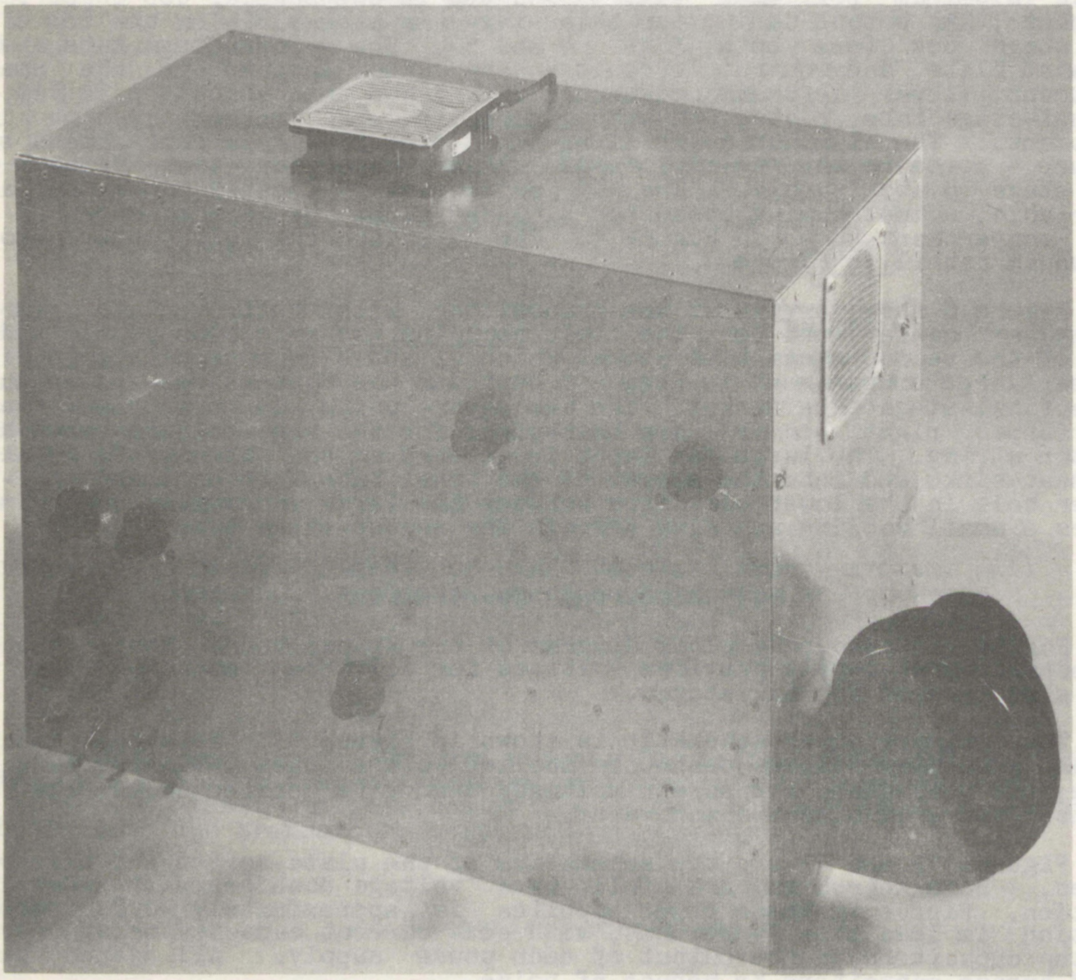

Figure 2. Front view of transmitter.

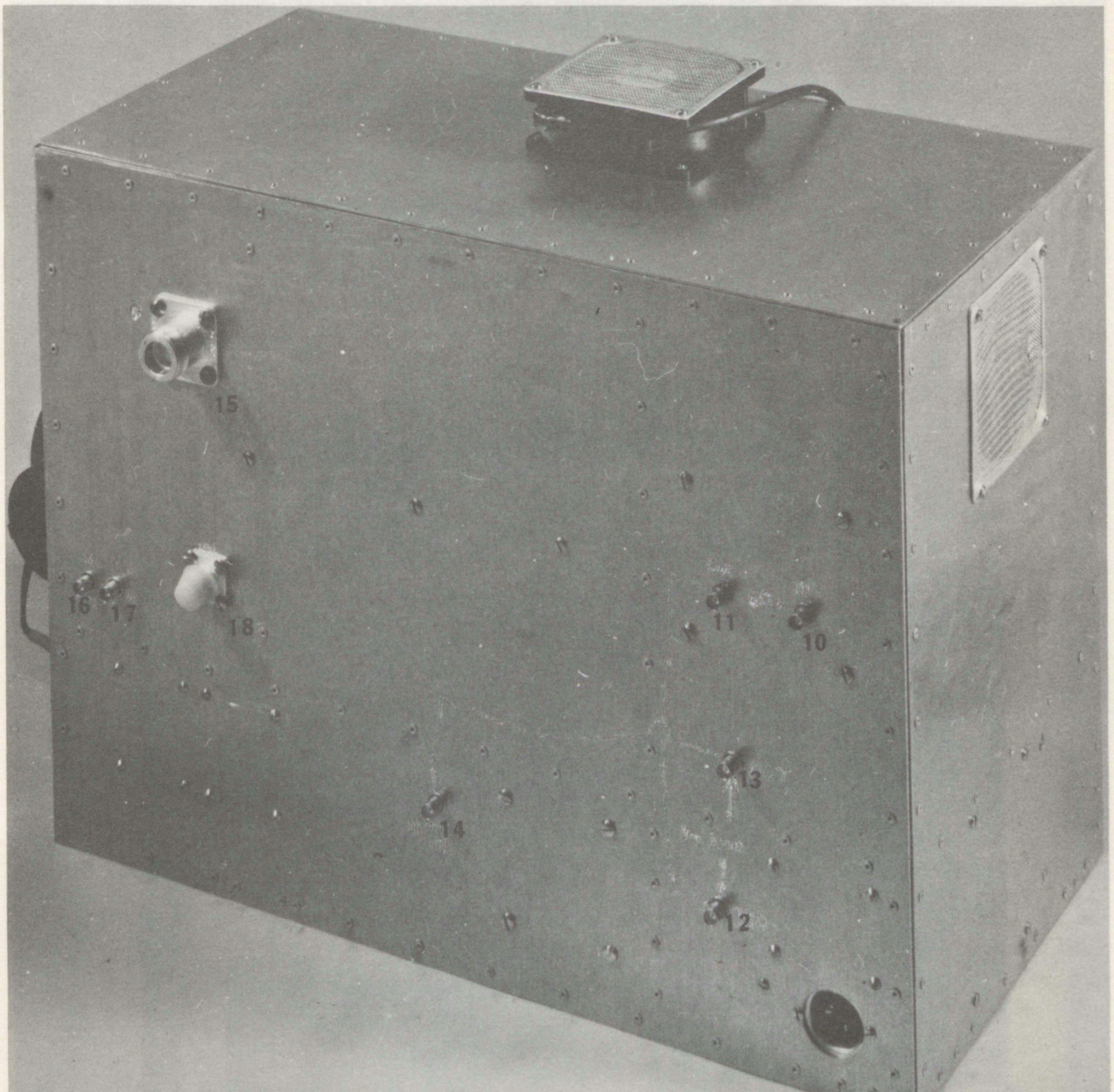

Figure 3. Back view of transmitter.

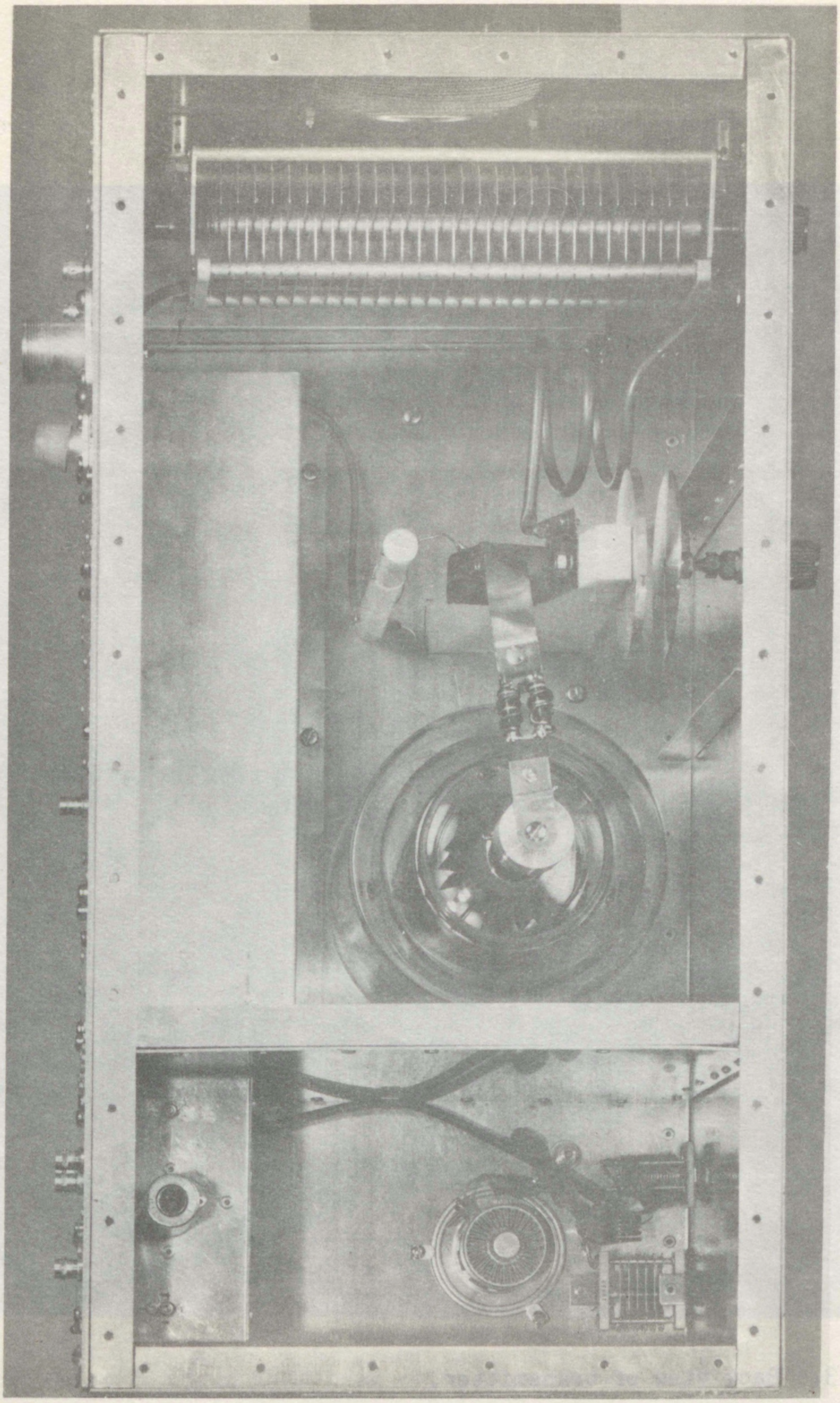

Figure 4. Top view of transmitter. The front panel is at the right of the picture.

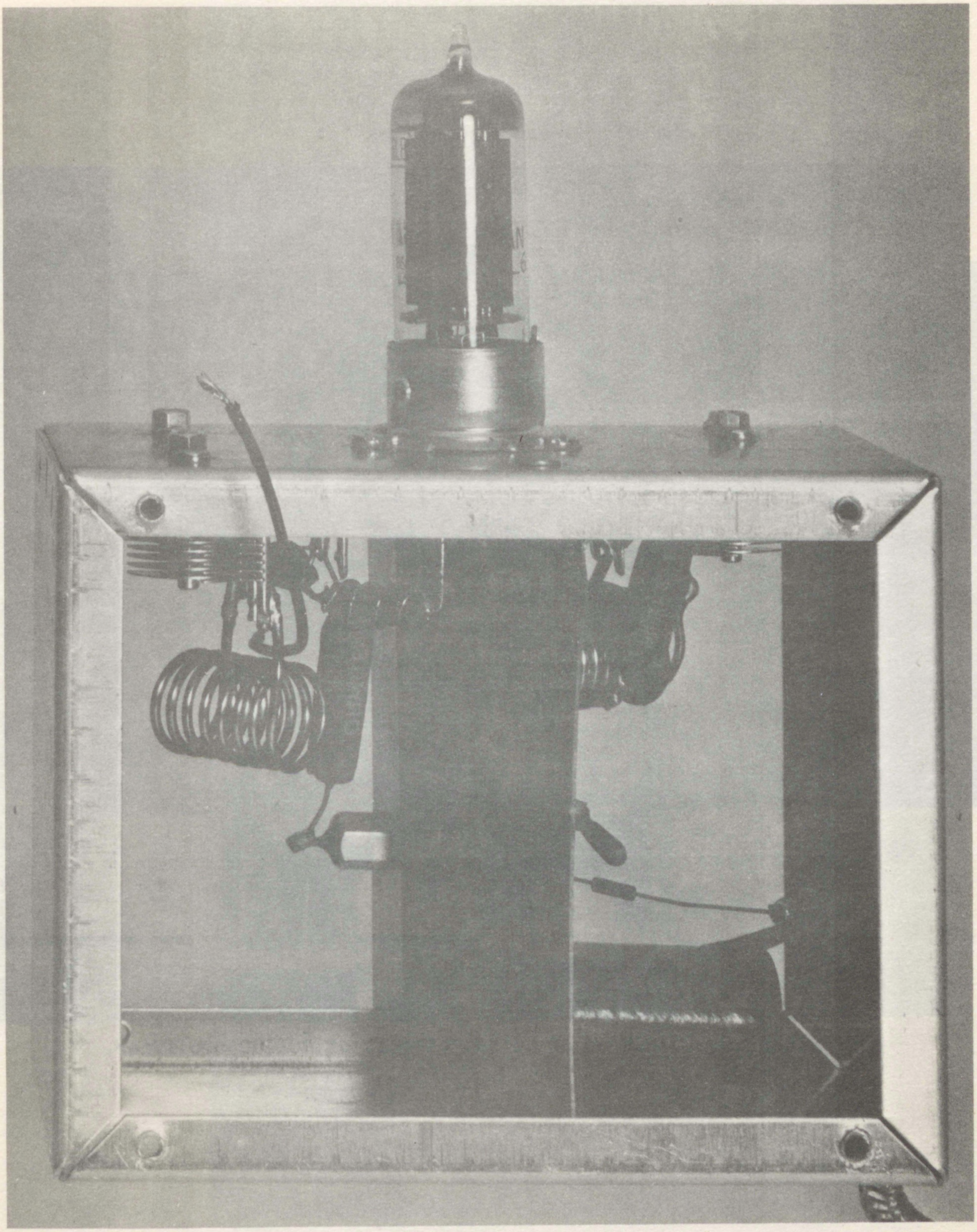

Figure 5. 6CL6 amplifier. The output circuitry is on the left side of the picture.

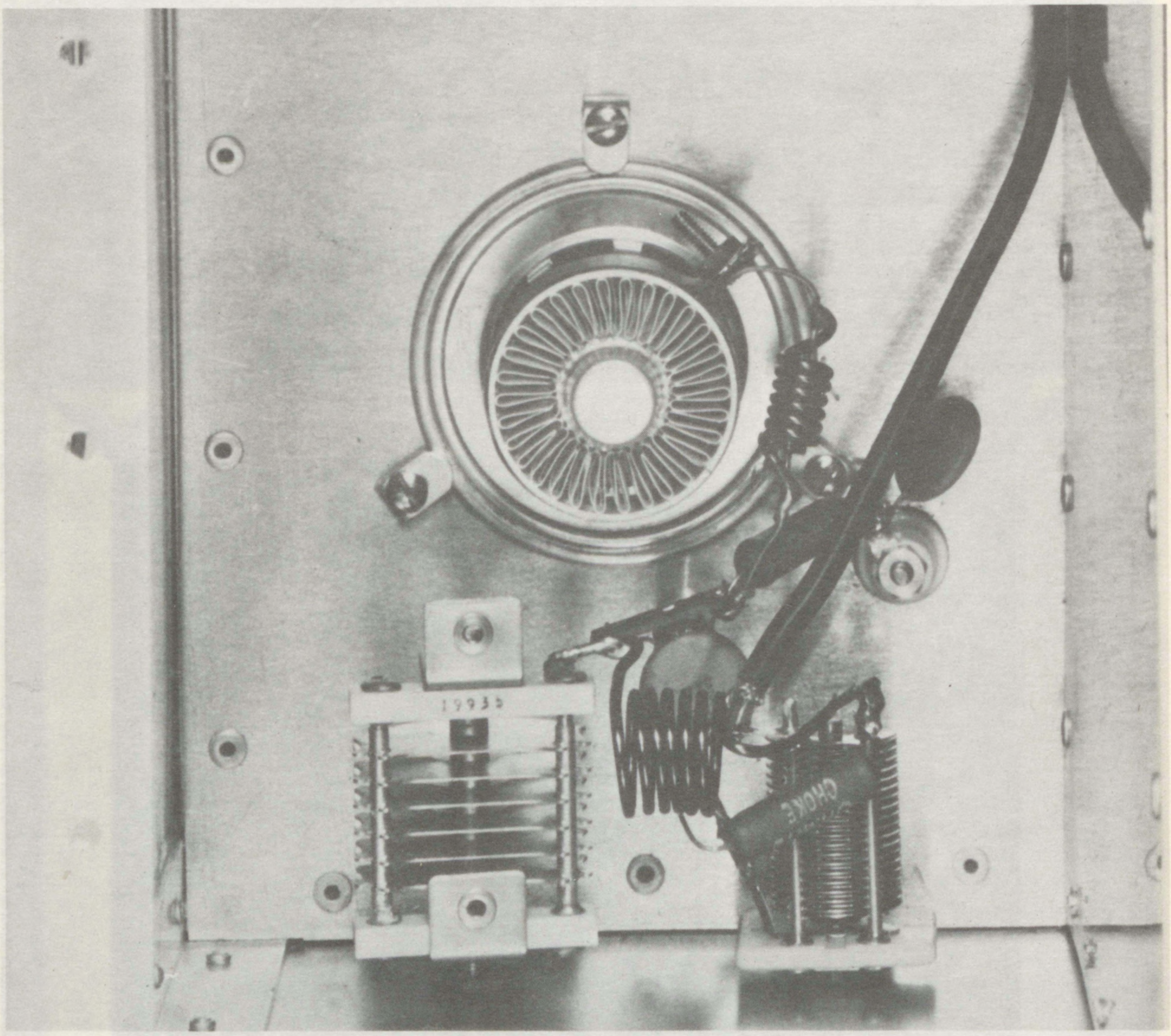

Figure 6. Close up of output circuit of 4CX250 amplifier.

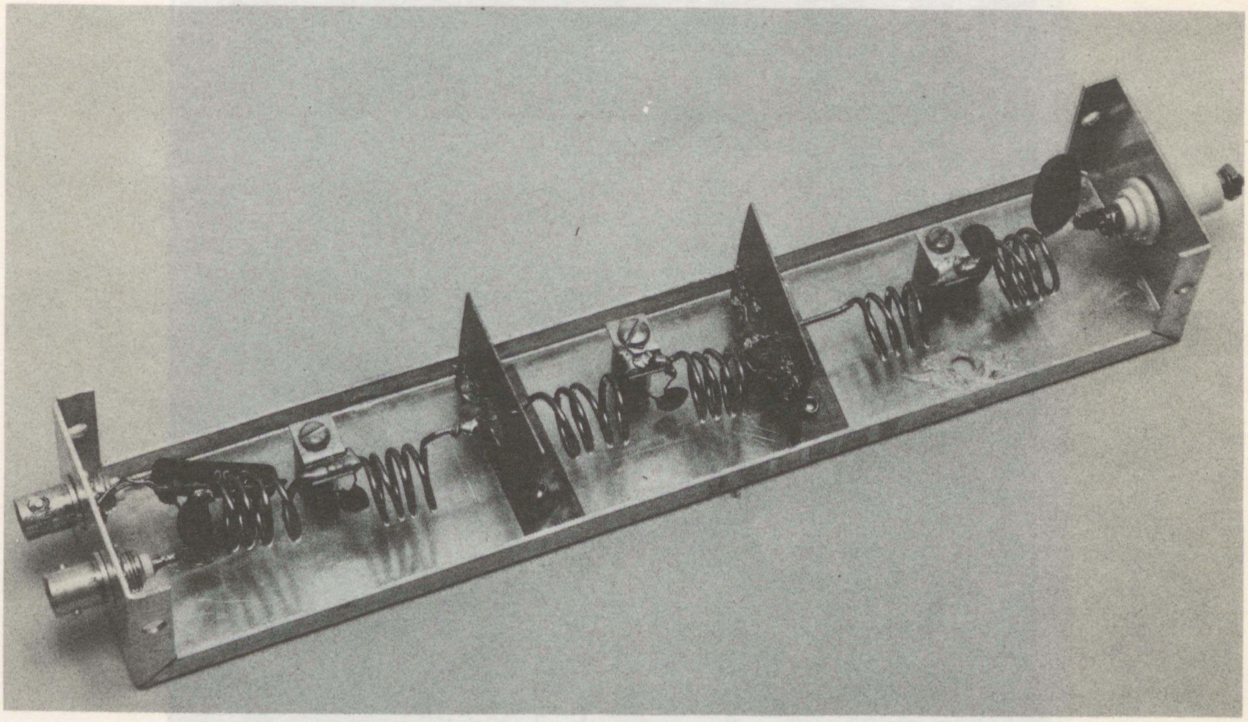

Figure 7. TR switch with the cover removed.

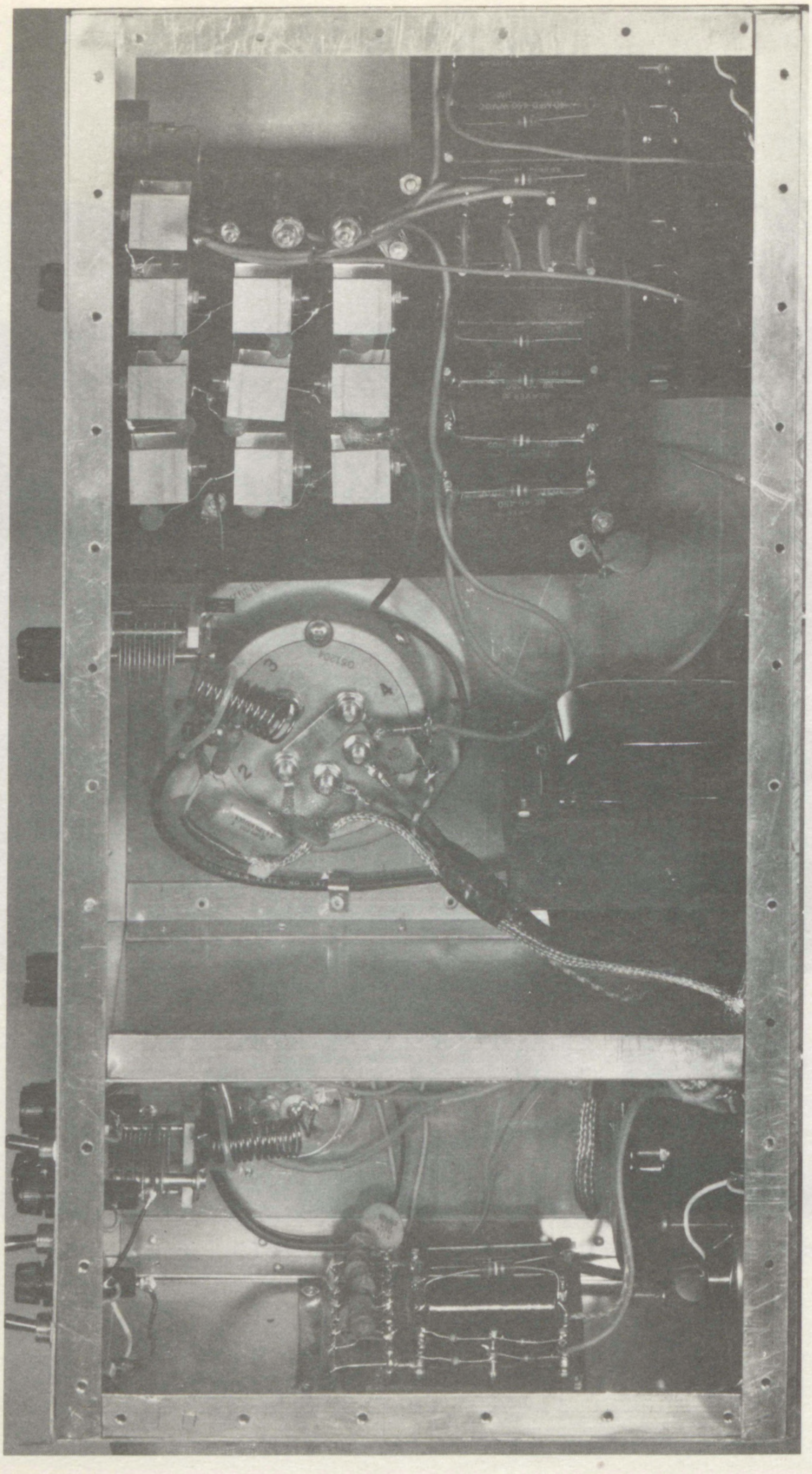

Figure 8. Bottom view of transmitter. The front of the transmitter is at the left of the picture.

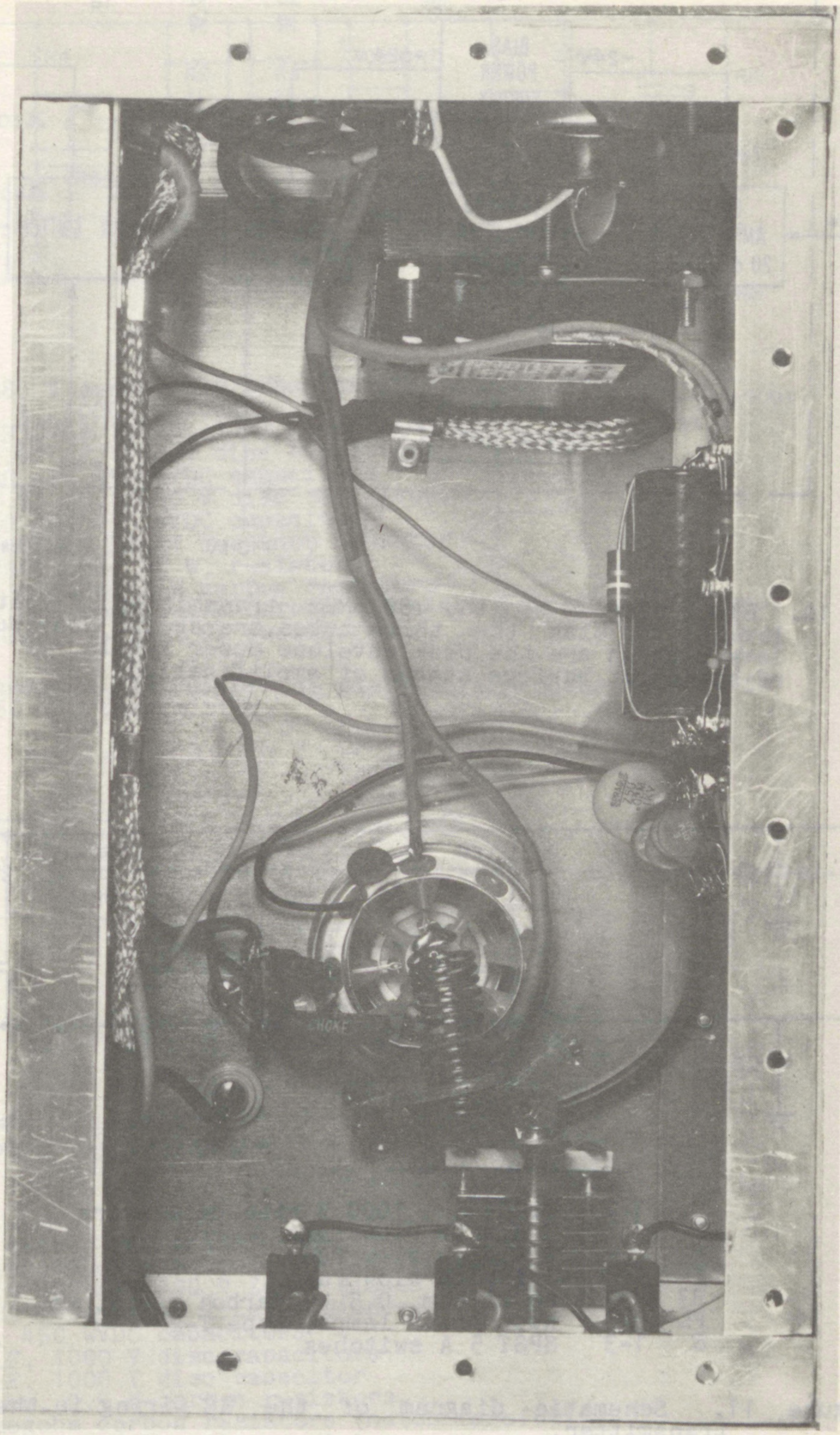

Figure 9. Close up of bottom of 4CX250 amplifier. The front panel is at the bottom of the picture. The bias power supply is visible along the right side of the transmitter.

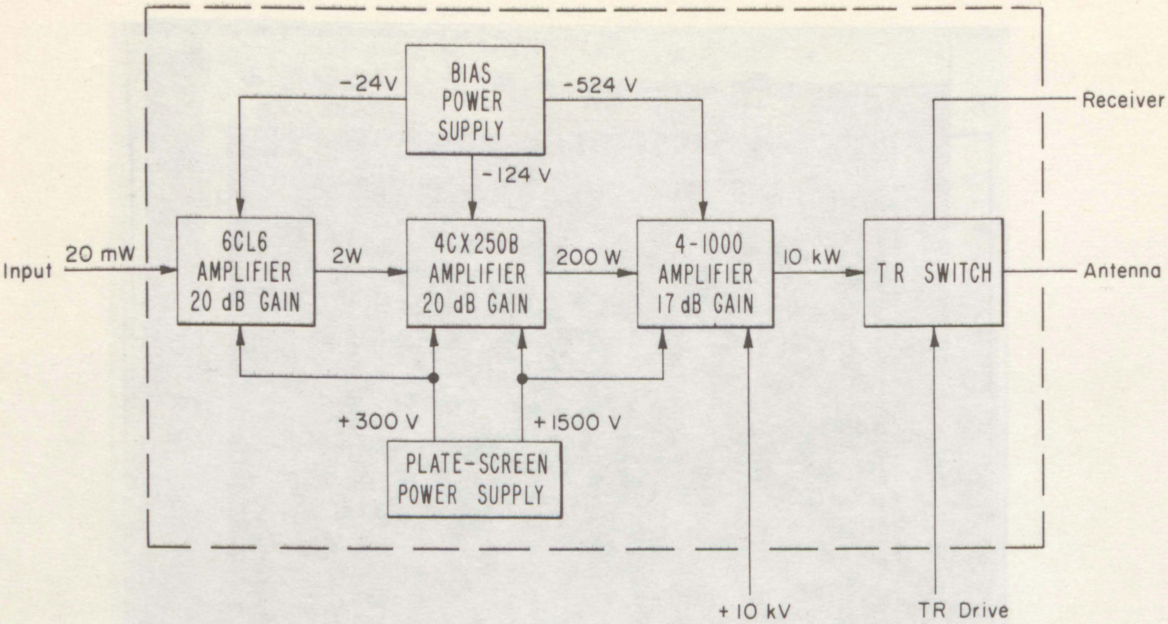

Figure 10. Block diagram of the 50 MHz transmitter. Voltage levels to bias the three tubes are shown. The power levels shown are the peak envelope power levels of the rf signal at various stages of amplification.

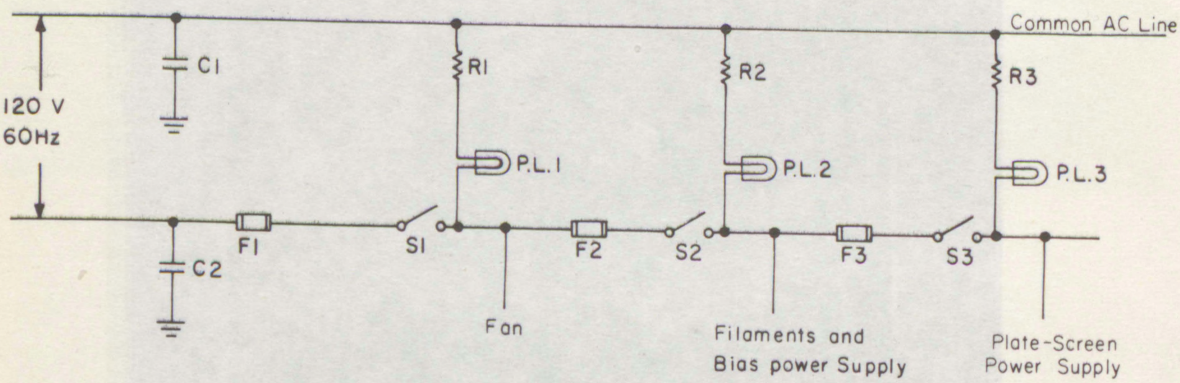

C	1-2	0.004 μF, 1000 V disc capacitors
F	1	3 A slow blow fuse
F	2	2 A slow blow fuse
F	3	1 A slow blow fuse
R3	1-3	68 kilohm, 0.5 W, carbon resistors
PL	1-3	Neon pilot lamps, type T-2
S	1-3	SPST 5 A switches

Figure 11. Schematic diagram of the AC wiring in the 50 MHz transmitter.

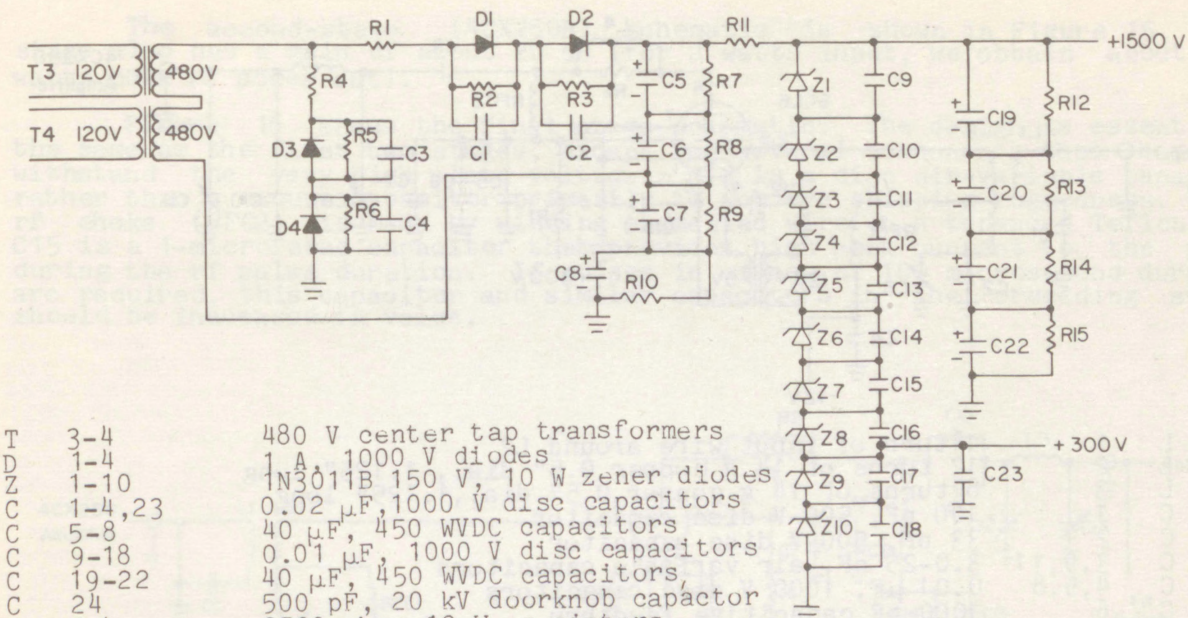

T	3-4	480 V center tap transformers
D	1-4	1 A, 1000 V diodes
Z	1-10	1N3011B 150 V, 10 W zener diodes
C	1-4,23	0.02 μF,1000 V disc capacitors
C	5-8	40 μF, 450 WVDC capacitors
C	9-18	0.01 μF, 1000 V disc capacitors
C	19-22	40 μF, 450 WVDC capacitors,
C	24	500 pF, 20 kV doorknob capacitor
R	1,4	2500 ohm, 10 W, resistors
R	2,3,5,6	1 megohm, 2 W carbon resistors
R	7-10,12-15	0.56 megohm, 1 W carbon resistors (carefully matched)
R	11	10 kilohm, 12 W, resistor

Figure 12. Schematic diagram of the plate-screen power supply in the 50 MHz transmitter.

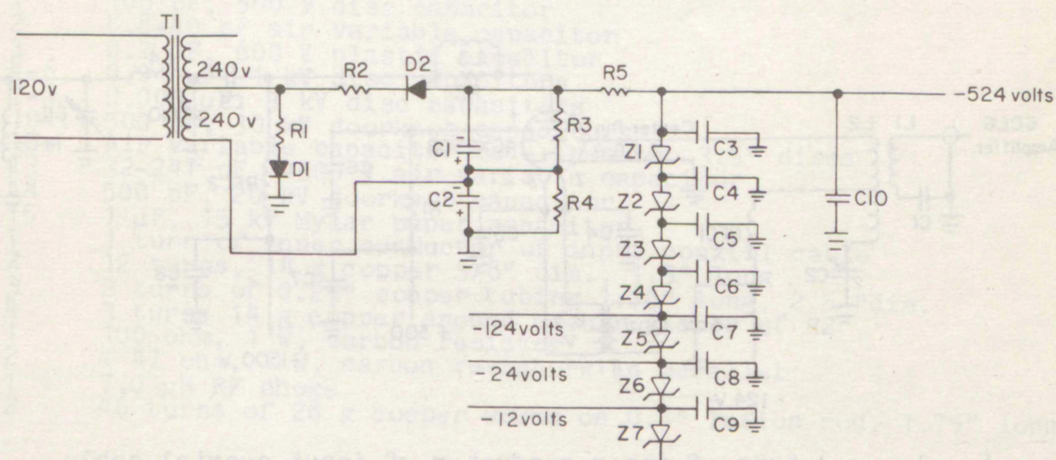

T	1	480 V center tap transformer
D	1-2	1 A, 1000 V diodes
Z	1-5	1N5271A 500 mW, 100 V Zener diodes
Z	6-7	1N5242A 500 mW, 12 V Zener diodes
C	1-2	40 μF, 450 WVDC capacitors
C	3-9	0.01 μF, 1000 V disc capacitors
C	10	0.02 μF, 1000 V disc capacitor
R	1-2	2 kilohm, 0.5 W carbon resistors
R	3-4	0.56 megohm carbon resistors (match carefully)
R	5	33 kilohm, 0.5 W carbon resistor

Figure 13. Schematic diagram of the 500 volt bias power supply.

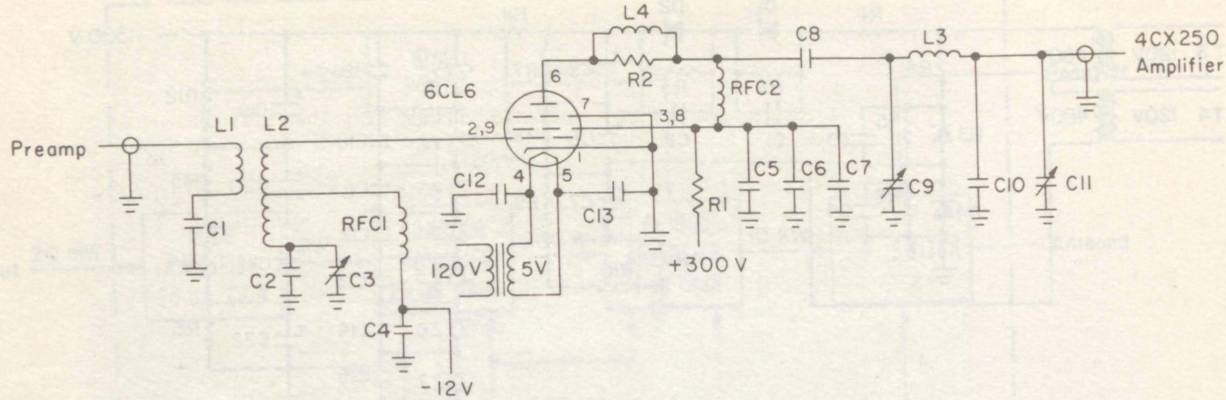

L	1	1 turn of input wire around L2
L	2	12 turns of 14 g copper 0.5" dia., 1.125" long
L	3	8 turns of 14 g copper 0.5" dia., 1.125" long
C	1	100 pF, 500 V disc capacitor
C	2	33 pF, 500 V disc capacitor
C	3,9,11	3.0-25 pF, air variable capacitors
C	4,5,8	0.01 μF, 1000 V disc capacitors
C	6	1000 pF capacitive feedthru
C	7	8 μF, 500 WVDC, capacitor
C	10	120 pF, 500 V disc capacitor
C	12,13	0.004 μF, disc capacitors
RFC	1,3	7.0 μH RF chokes
RFC	2	3 turns 20 g copper around a 100 ohm resistor
T	1	5 V windings of transformer in the 500 V bias power supply

Figure 14. Schematic diagram of 6CL6 amplifier.

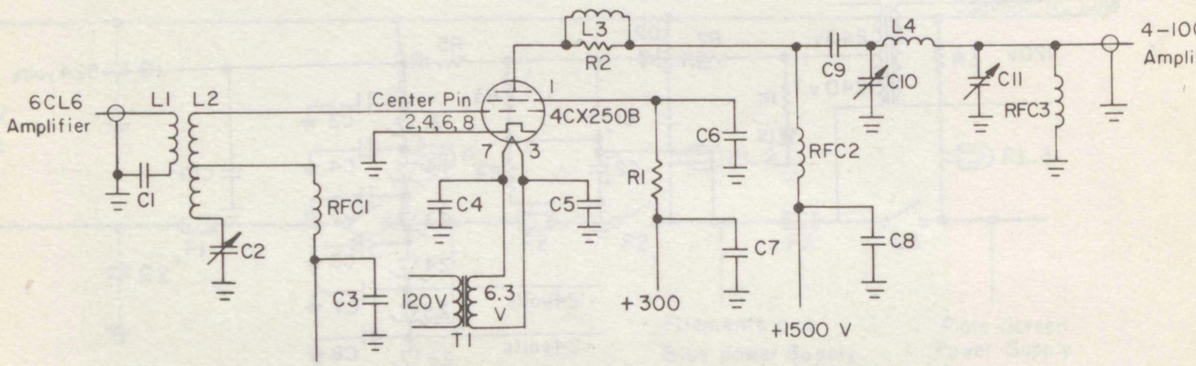

L	1	1 turn of inner conductor of input coaxial cable
L	2	14 turns of 14 g copper 0.5" dia., 1.5" long
L	3	6 turns of 14 g copper wound on R2
L	4	6 turns of 14 g copper 5/8" dia., 0.75" long
C	1	100 pF, 500 V disc capacitor
C	2,10	8.8-40 pF, air variable capacitors
C	3-7	0.01 μF, 1000 V ceramic disc capacitors
C	8-9	0.005 μF, 3 kV disc capacitors
C	11	90-140 μF, air variable capacitor
RFC	1-3	7.0 μH RF chokes
T	1	6.3 V windings of transformer in the 500 V bias power supply
R	1	510 ohm, 1 W carbon resistor
R	2	56 ohm, 1 W carbon resistor

Figure 15. Schematic diagram of the 4CX250 amplifier.

The second-stage (4CX250B) schematic is shown in Figure 15. This stage also has a gain of about 20 dB (for 2 watts input, we obtain about 200 watts peak rf power out).

Figure 16 shows the final stage schematic. The design is essentially the same as the first two stages, except for several components that have to withstand the very high plate voltage. C12 is a disc air-variable capacitor rather than a vacuum capacitor primarily to achieve shipping ruggedness. The rf choke (RFC2) is made by winding enamelled wire on a threaded Teflon rod. C15 is a 1-microfarad capacitor that provides high peak current to the plate during the rf pulse duration. If pulses in excess of 100 microsecond duration are required, this capacitor and similar capacitors in the preceding stages should be increased in value.

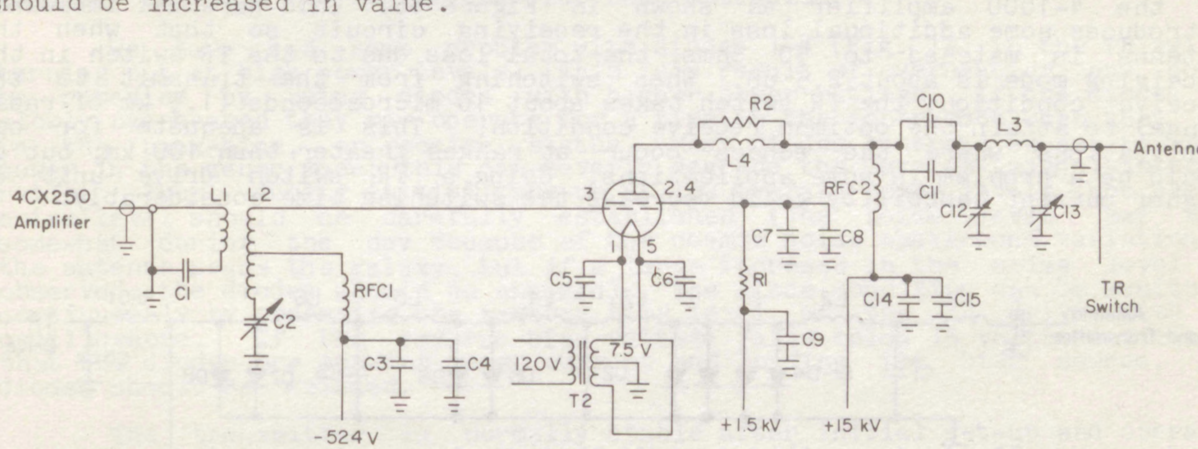

T	2	7.5 V, 22 A filament transformer
C	1	100 pF, 500 V disc capacitor
C	2	8.8-40 pF air variable capacitor
C	3	0.2 μF, 600 V plastic capacitor
C	4-6	0.01 μF, 1 kV disc capacitors
C	7-9	0.005 μF, 3 kV disc capacitors
C	10-11	500 pF, 30 kV doorknob capacitors
C	12	Air variable capacitor made from two 3.5" discs
C	13	32-241 pF, 4500 V air variable capacitor
C	14	500 pF, 20 kV doorknob capacitor
C	15	1 μF, 15 kV Mylar paper capacitor
L	1	1 turn of inner conductor of input coaxial cable
L	2	12 turns, 14 g copper 5/8" dia., 1.5" long
L	3	2 turns of 0.25" copper tubing 1.75" long, 2.5 "dia.
L	4	3 turns 14 g copper around each resistor of R2
R	1	100 ohm, 1 W, carbon resistor
R	2	4 47 ohm, 1 W, carbon resistors in parallel
RFC	1	7.0 μH RF choke
RFC	2	46 turns of 28 g copper wound on 0.5" Teflon rod, 1.75" long

Figure 16. Schematic diagram of the 4-1000 amplifier.

2.4 Transmit-receive (TR) switch

Figure 17 shows the schematic of the TR switch shown in Figure 7. The system synchronizer (Fig. 1) applies about 60 mA of forward bias current to the TR switch about 10 microseconds before the diode switch is turned on to pass an rf pulse from the crystal oscillator to the transmitter. During the forward biased period, the signal at the receiver terminal (Fig. 17) is about 66 dB below the peak rf power level of the transmitter. About 10 microseconds after the transmitter rf pulse ends, the TR switch diodes are again back biased at 15 volts. In this configuration the 3-element Tee filter has an insertion loss of only about 1.8 dB. Since no anti-transmit-receive (ATR) switch is used, the receiver is essentially in parallel with the output cicuit of the 4-1000 amplifier as shown in Figure 16. This parallel impedance introduces some additional loss in the receiving circuit so that when the antenna is matched to 50 ohms, the total loss due to the TR switch in the receiving mode is about 2.5 dB. When switching from the transmit to the receive condition, the TR switch takes about 10 microseconds (1.5 km of radar range) to attain the optimum receive condition. This is adequate for our applications where the echoes occur at ranges greater than 100 km, but it could be a problem in some applications. Using a TR switch drive unit of higher current capability would decrease the switching time considerably.

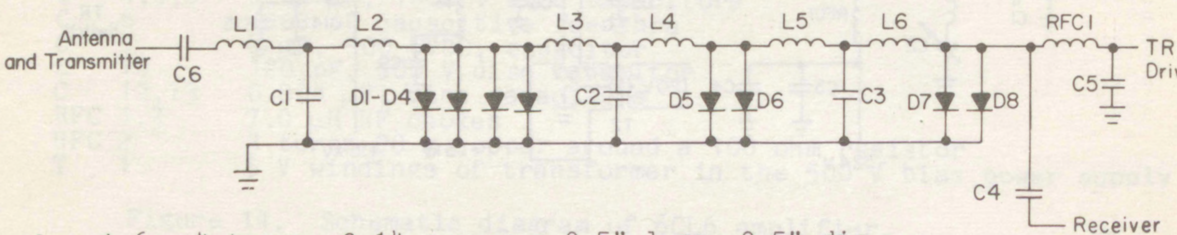

L	1-6	4 turns of 14 g copper 0.5" long, 0.5" dia.
C	1	50 pF, 6000 V disc capacitor
C	2-3	50 pF, 500 V disc capacitors
C	4-5	0.01 μF, 100 V disc capacitors
C	6	0.005 μF, 3000 V disc capacitor
D	1-8	1 A, 1000 V diodes
RFC	1	7.0 μH RF choke

Figure 17. Schematic diagram of the TR switch.

2.5 Transmitter operation and performance

To put the transmitter into operation the fans are turned on first, then the filaments and bias supply, and finally the plate-screen power supply. After filament warm-up, the final stage plate voltage is applied. If the transmitter is being excited by the crystal oscillator/diode switch source, care should be taken to see that the TR switch is being driven so that the TR diodes and the receiver input are protected when the transmitter is put into operation. A 60 dB directional coupler is normally installed on the transmitter output and the sidearm signal is fed to an oscilloscope with a frequency response of at least 50 MHz. The oscilloscope sweep is normally triggered from the system synchronizer and starts when the TR switch is forward biased. This allows the entire rf pulse to be displayed on the screen, and tuning each stage for peak rf power output can be easily accomplished. In addition, the 50-MHz waveform can be examined for harmonic content and the plate tuning adjusted to minimize distortion while maximizing power output. Normal procedure is to set the plate voltage at about 5 kV for initial tuning. After each stage is tuned, the plate voltage can be raised to the desired level. After a large increase in plate voltage it may be necessary to slightly retune the final plate and output circuit for optimum results.

It is possible to detune the transmitter to a point where oscillation will occur. This normally causes the final-stage plate supply to draw overcurrent and trips the overload relay. This oscillation can also damage the TR circuitry . The oscillation problem could probably be greatly reduced by providing a double cabinet around the final output stage. This would reduce the circulating rf currents in the outer transmitter case which currently provide a path for feedback so that oscillation can occur. In normal operation we have found that after initial tune-up, oscillation is no problem, but the reader should be aware of this design weakness. In addition, proper operation can be difficult if the antenna is too near the transmitter. This allows the large radiated signal to feed back into preceding stages and cause distortion and oscillation. In general, the antenna should be several hundred feet from the transmitter for best operation.

We have had some problem with diodes 1-4 (Fig. 17) in the TR switch burning out at high power levels. This is a result of overheating, and could be remedied by using diodes with higher power ratings. If the diodes are slowly overheated they may operate for a time in the zener mode when they are in the back-bias, or receive, status. Most diodes generate excess rf noise power in the zener mode; this can severly degrade the system signal-to-noise ratio. Thus, during initial tune-up at low average power levels, the system noise level should be carefully established (The noise level may vary somewhat during the day because of the cosmic noise background variation as the antenna scans the galaxy, but if a large increase in the noise level is observed, the diodes should be checked). The diode condition can be monitored continuously by observing the reverse bias level of the TR drive with an oscilloscope. If the reverse bias voltage falls below 15 volts, indicating that the diodes are drawing zener current and loading the bias source, the diodes should be replaced.

The transmitter is normally stable after initial set-up and operates reliably at plate voltages of about 10 kV, providing about 15 kW peak rf power. The rise time of the rf pulse out of the transmitter is about 0.5 microsecond. The transmitter efficiency is about 75 percent and could be improved by enclosing the third-stage plate circuit in a separate box inside the transmitter case. Although the transmitter could be improved, the design presented here has been adequate for our needs.

3. DIODE SWITCH

As indicated in Figure 1, the transmitter is excited by the crystal oscillator. The diode switch, under control of the system synchronizer, passes an rf pulse from the crystal oscillator to the preamplifier, which drives the transmitter. While the crystal oscillator, diode switch, and preamplifier are all contained in the frequency coherent receiver unit, the diode switch is described here because of its importance in attaining a good Doppler radar system. The most important feature of the switch is that it must provide very high isolation in the off (receive) condition. The reason for this isolation requirement is that the transmitter output is in parallel with the antenna in the receive condition. Since a low level rf signal at the input of the transmitter will only be attenuated by 20 dB at the output, the crystal oscillator must be well isolated from the transmitter during reception. In order to reduce the crystal oscillator signal to an acceptable level, at least 120 dB of isolation is needed in the diode switch. In our design the isolation is about 140 dB.

Figure 18 shows the crystal oscillator and diode switch box. As shown in Figure 19, the diode switch consists of two 5-diode "layers". Care has been taken to filter the crystal oscillator signal from leaking out on power supply leads, switch drive leads, etc. The crystal oscillator module is under the diode switch section mounted in the larger box. A schematic of the diode switch is shown in Figure 20.

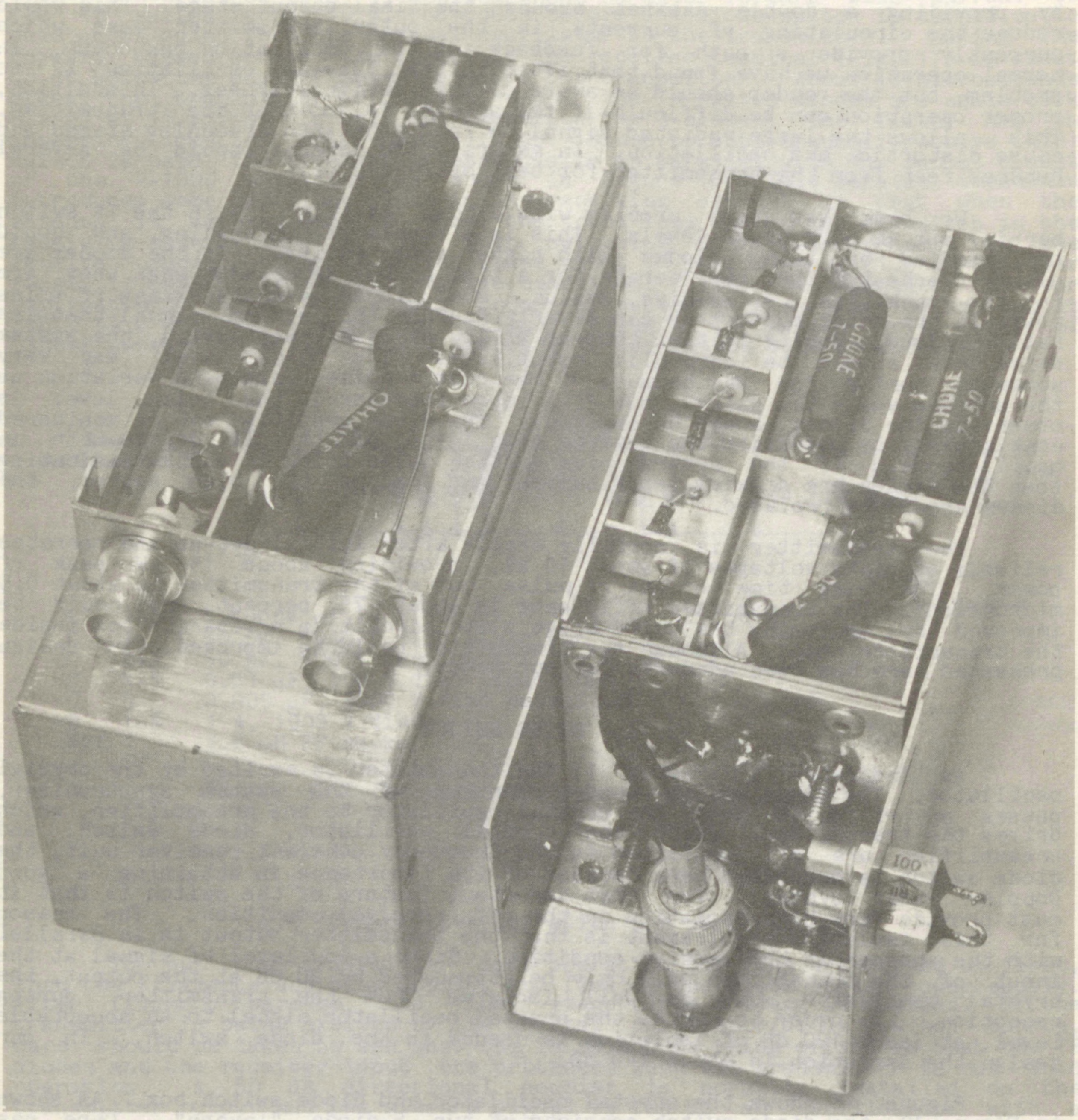

Figure 18. The diode switch with covers taken off.

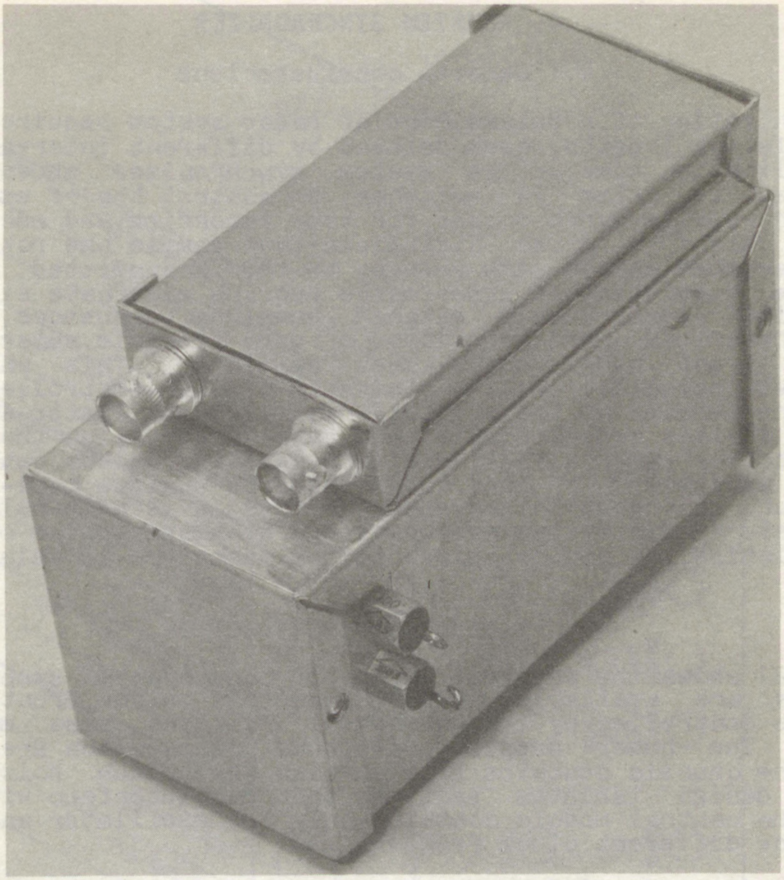

Figure 19. Diode switch with cover on. Note how the two utility boxes are mounted piggyback.

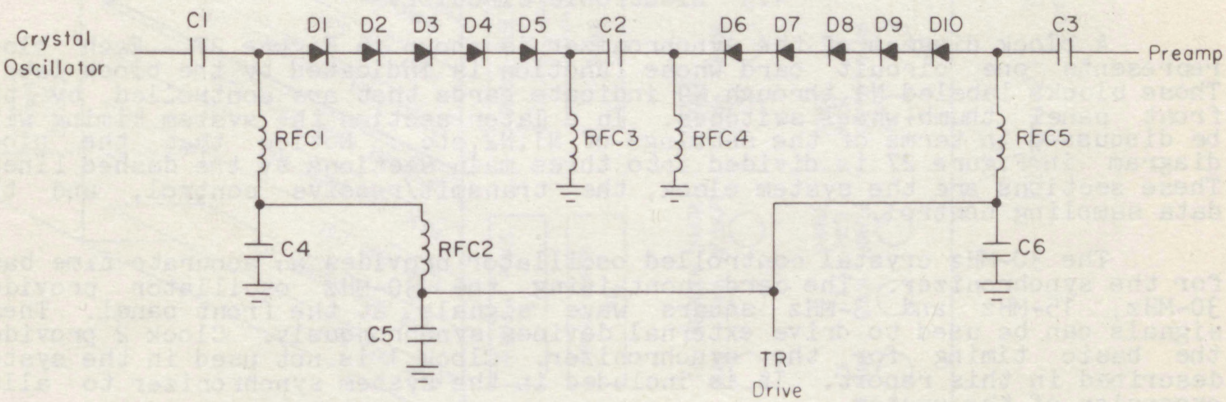

RFC 1-5 7.0 μH RF chokes
C 1-3 0.005 μF disc capacitors
C 4-6 0.001 μF disc capacitors
D 1-10 1N270 diodes

Figure 20. Schematic diagram of the diode switch.

4. SYSTEM SYNCHRONIZER

4.1 General considerations

Synchronization of a pulsed Doppler radar system requires a number of pulses of different lengths, each delayed by different intervals with respect to some initialization time. The system synchronizer shown in Figure 1 provides pulses to drive TR switches, to control the rf excitation of the transmitter, to provide synch pulses for tape recording and oscilloscope sweep triggers, and also to drive digitizers that sample the returned signal at accurately determined delays with respect to the transmitted rf pulse. In addition, more sophisticated experiments require alternate single and double rf pulses, with appropriately matched sampling sequences. The system synchronizer described here provides a very flexible pulse format that is controlled by front panel thumb-wheel switches. This unit is rugged, well-shielded electrically, and the timing is crystal-controlled for accuracy. Sub-multiple frequencies of the crystal-controlled oscillator are available to drive external devices synchtonously, and gate inputs allow the pulse sequence to be interrupted by external devices. The sampling pulses can be used for on-line data analysis, or they can be used to analyze tape-recorded analog data on playback. Although this system provides a single-pulse/double-pulse option, a basic radar system synchronizer for single-pulse operation can be realized by deleting the double-pulse options described in this report.

4.2 Mechanical construction

Figure 21 shows the physical layout of the system synchronizer. The various pulses are available at BNC connectors on the front panel, and the pulse format is controlled by the thumbwheel switches also mounted on the front panel. The power supplies, fan, and power switch are mounted on the back panel. The chassis contains five modules which each hold five circuit cards. This design isolates sections that may interfere with one another. For example, the central module contains only the oscillator and divider cards that provide the different clock frequencies.

Figures 22 and 23 are photographs of the front and back of the synchronizer. It is approximately 47 cm long, 15 cm high, and 30 cm deep, and is constructed of 1/8" irridited aluminum. The cooling fan draws air through the aluminum screen on the top of the unit. Figure 24 shows how the power supplies, fan, and power switch are mounted on the inside of the back panel. Figure 25 shows the backs of the thumbwheel switches on the front panel, the five modules, the card slots, and the 60-pin edge connector sockets for each circuit card. One of the 9 by 12 cm circuit cards is shown in Figure 26.

4.3 Electronic circuitry

A block diagram of the synchronizer is shown in Figure 27. Each block represents one circuit card whose function is indicated by the block label. Those blocks labeled N1 through N9 indicate cards that are controlled by the front panel thumb-wheel switches. In a later section the system timing will be discussed in terms of the settings of N1,N2,etc. Notice that the block diagram in Figure 27 is divided into three main sections by the dashed lines. These sections are the system clock, the transmit/receive control, and the data sampling control.

The 30-MHz crystal controlled oscillator provides an accurate time base for the synchronizer. The card containing the 30-MHz oscillator provides 30-MHz, 15-MHz and 3-MHz square wave signals at the front panel. These signals can be used to drive external devices synchronously. Clock 2 provides the basic timing for the synchronizer. Clock 1 is not used in the system described in this report. It is included in the system synchronizer to allow expansion of the system.

The transmit/receive section controls the pulse length (N2), pulse repetition frequency (N3), and the delay between double pulses (N6) when the double pulse option is being used. The transmitter can be stopped by an external device by use of the transmit interrupt line.

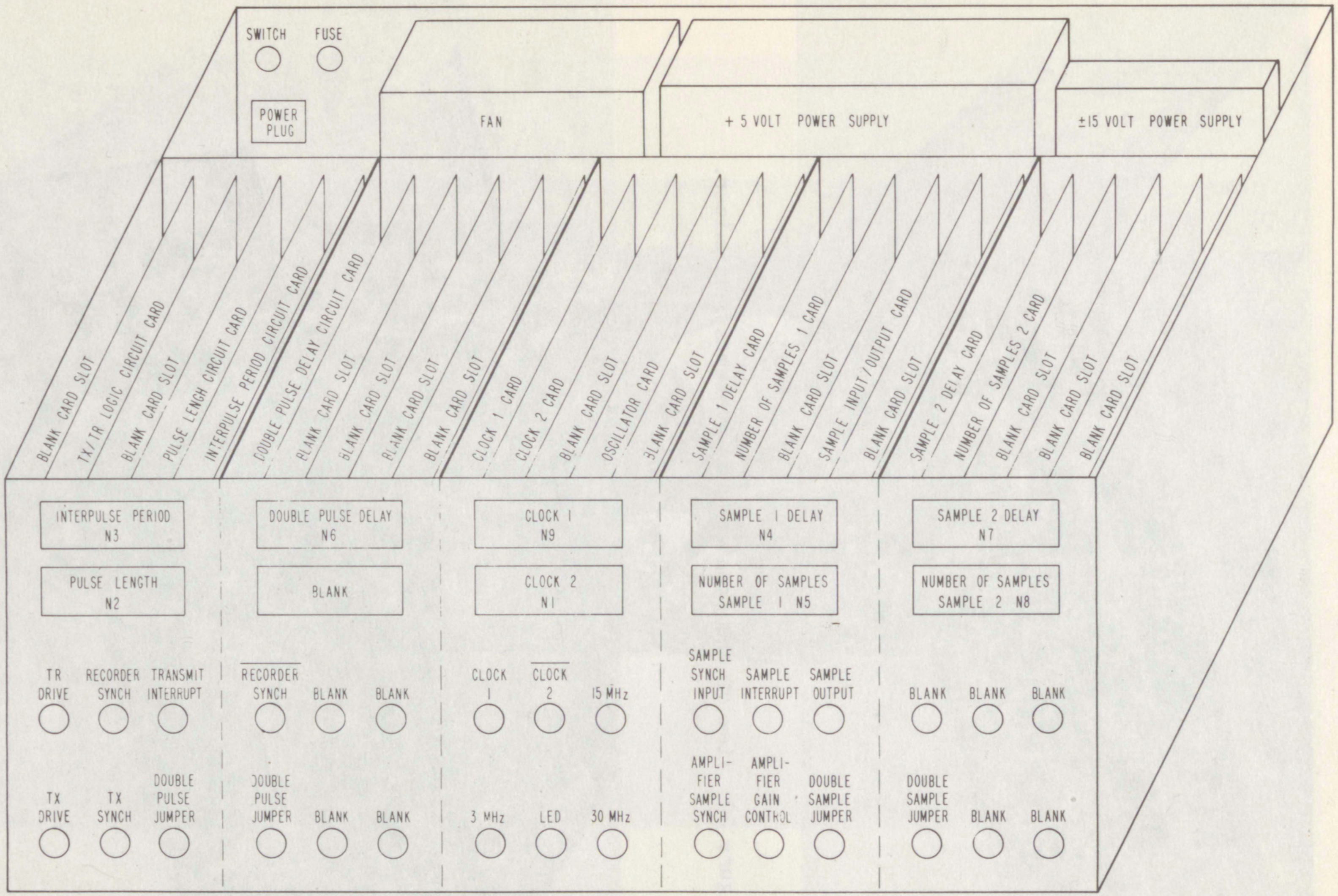

Figure 21. Physical layout of the system synchronizer, showing location of the output functions and circuits.

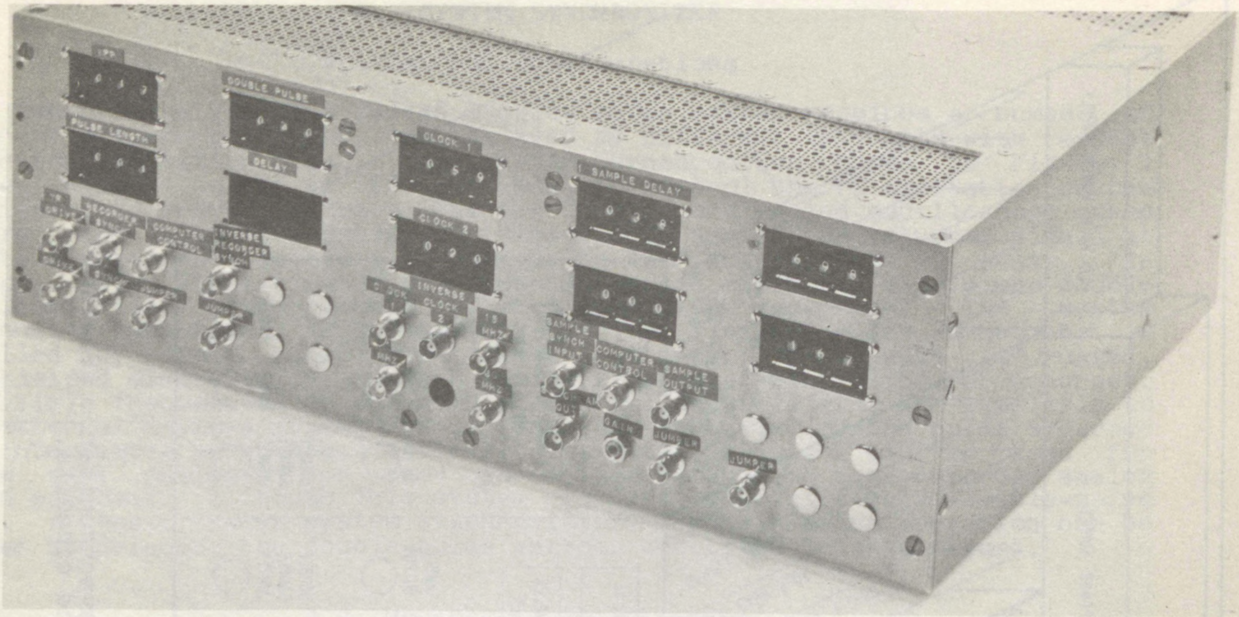

Figure 22. View of the front of the system synchronizer.

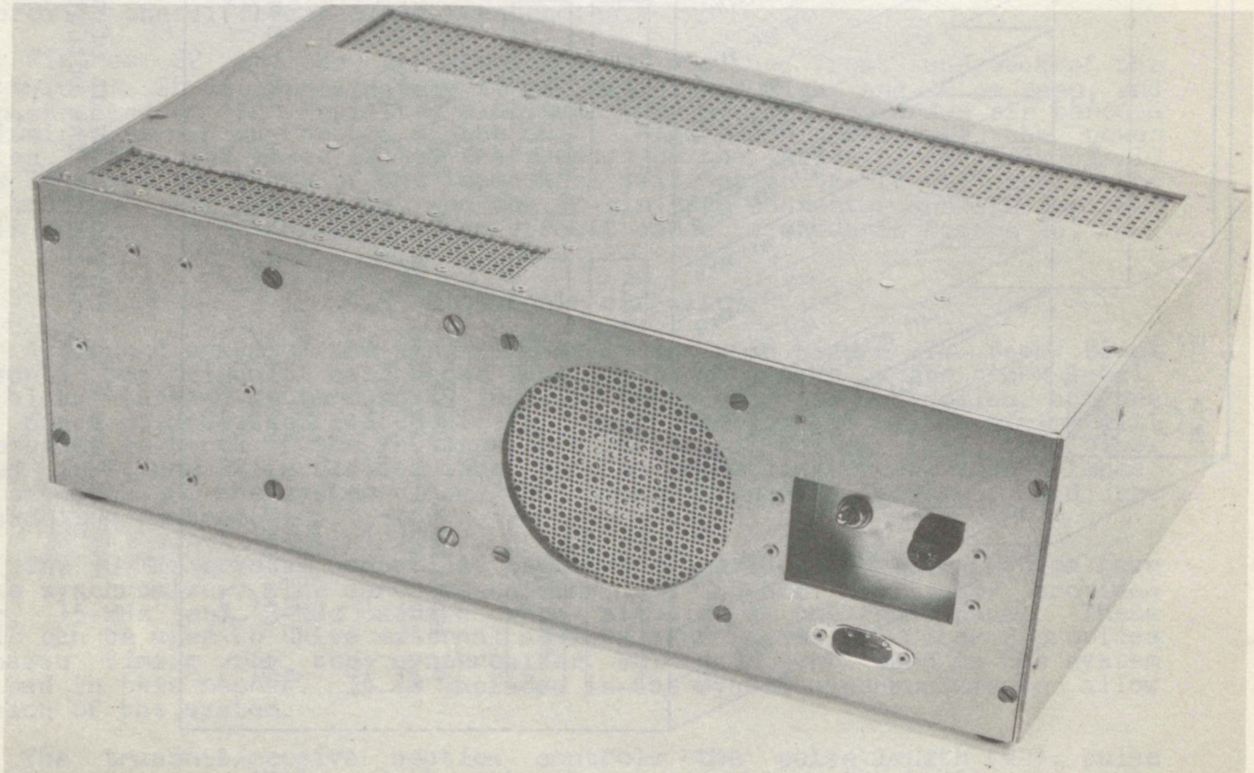

Figure 23. Rear view of the system sychronizer.

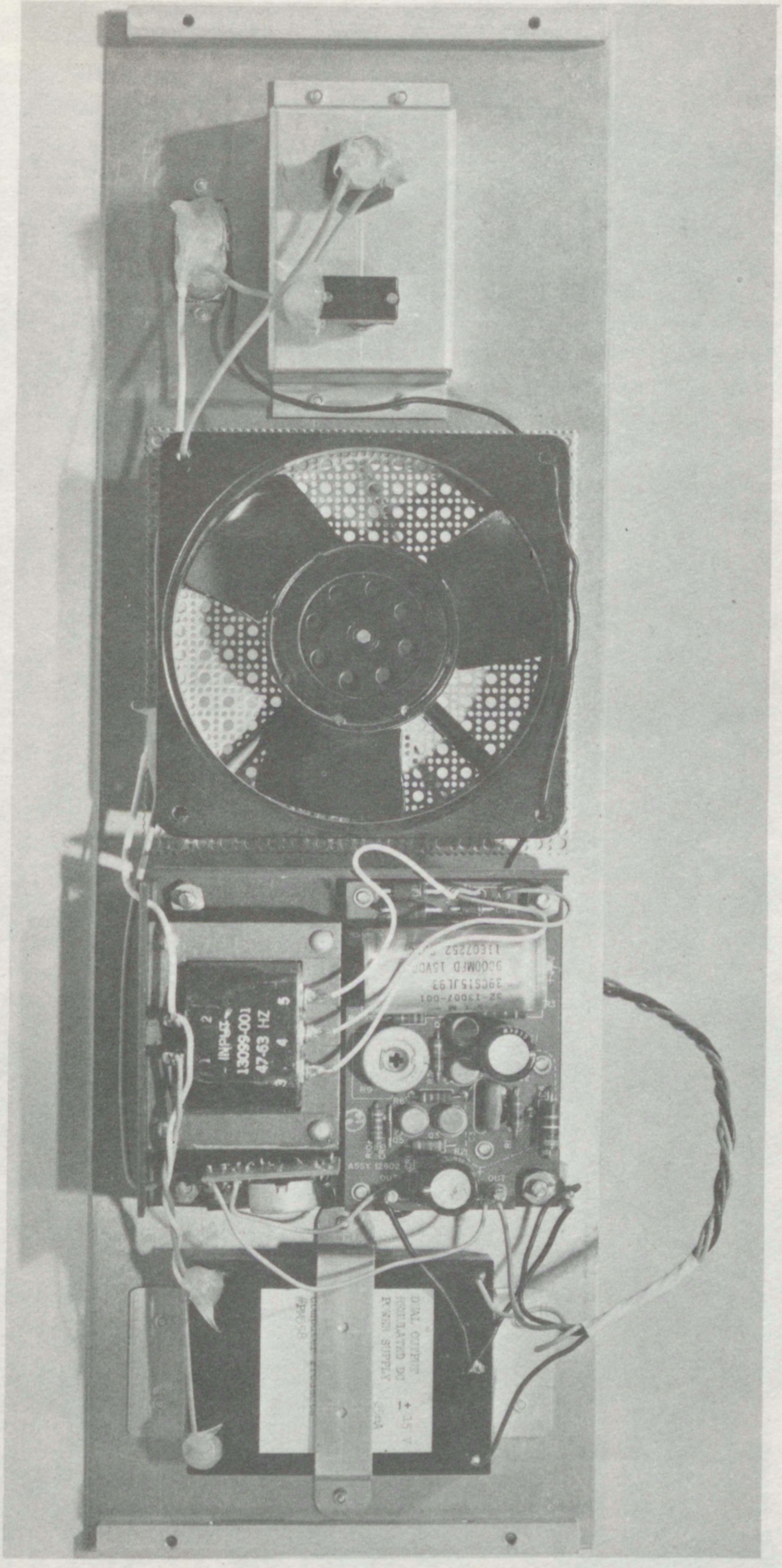

Figure 24. View of the back panel of the system synchronizer showing the switch, fan, and power supplies.

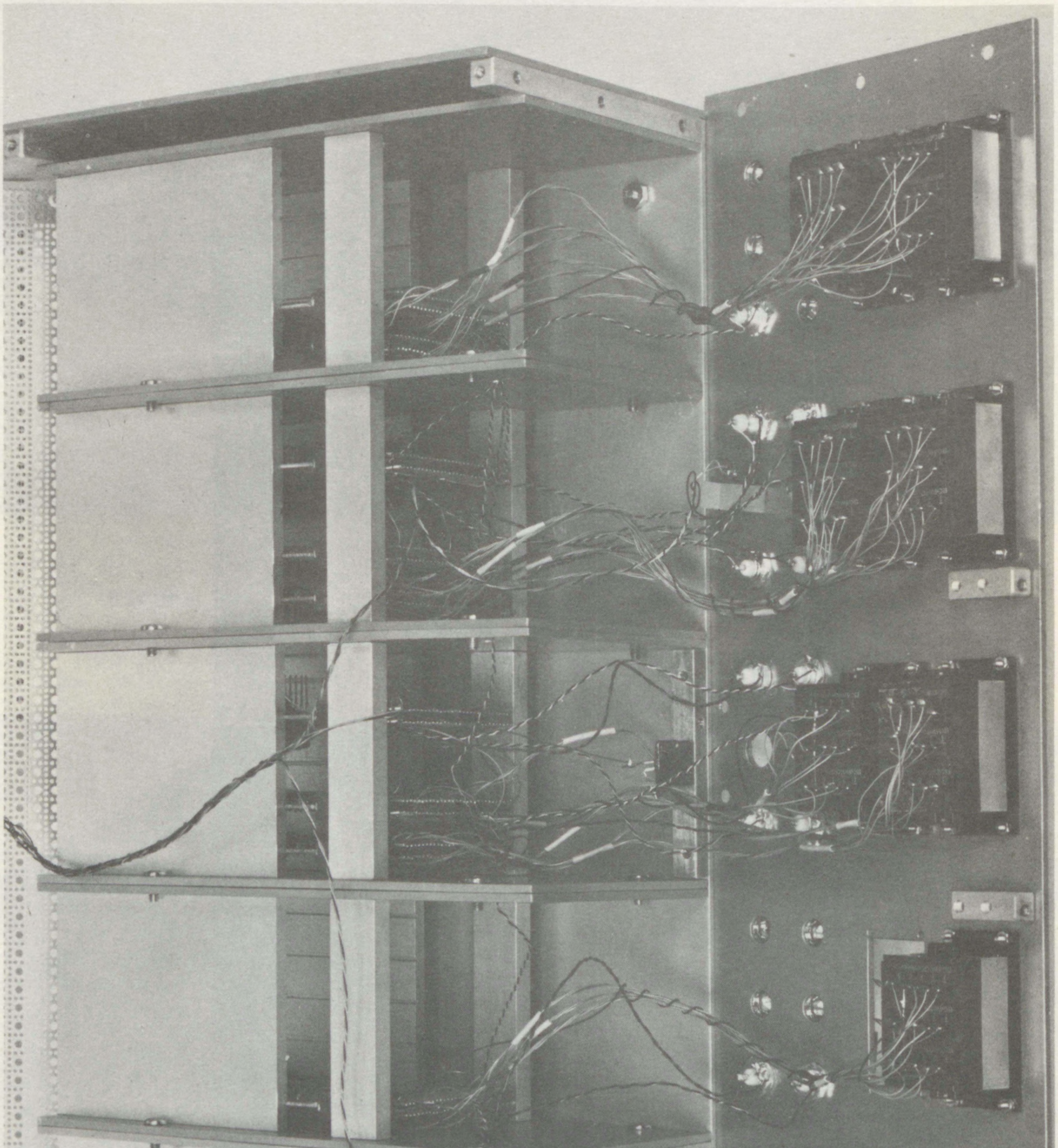

Figure 25. View of the system synchronizer with the top off and the front panel lowered.

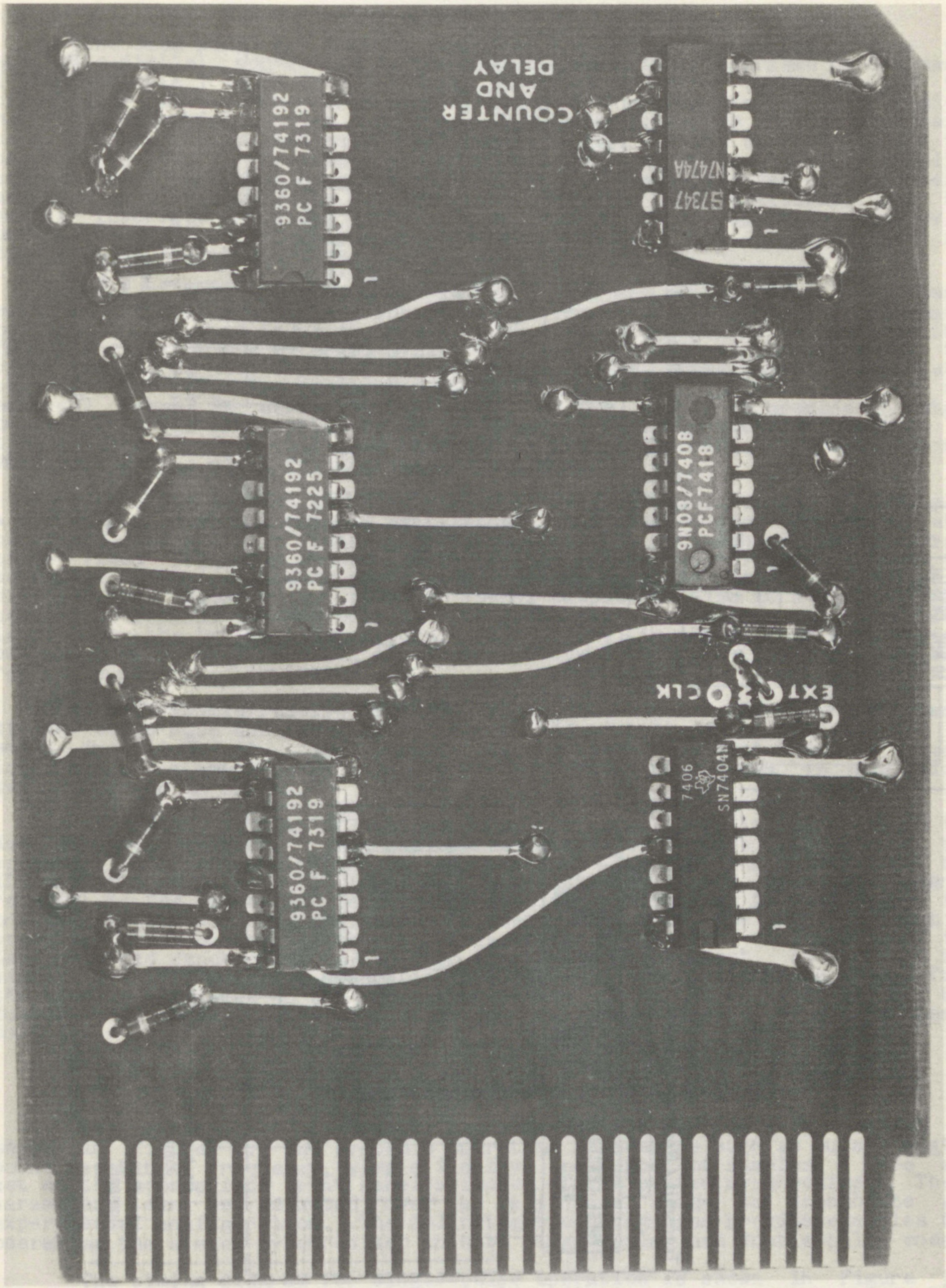

Figure 26. Basic circuit card.

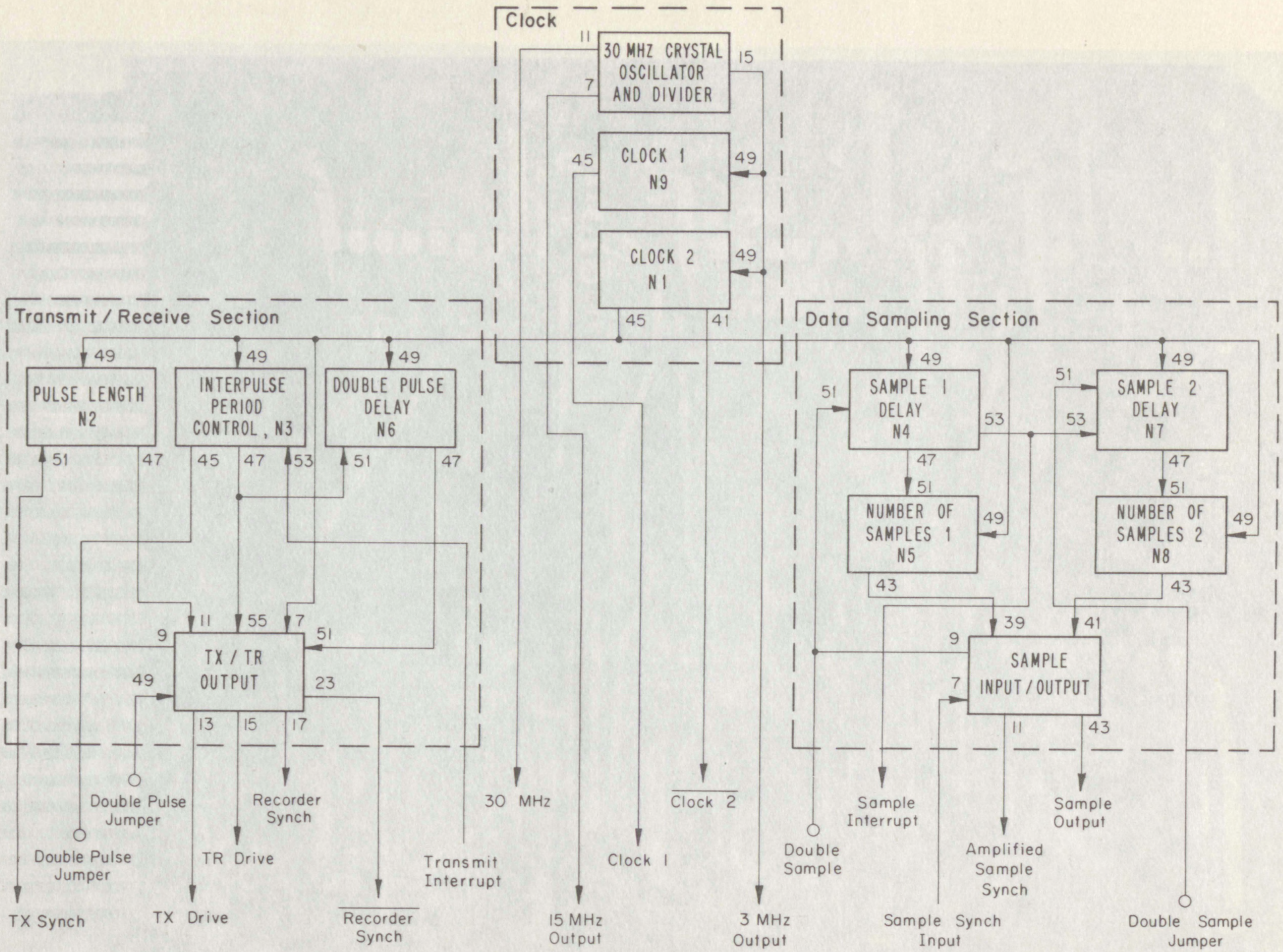

Figure 27. Block diagram of the system synchronizer.

The data sampling control section produces pulses that drive the analog-to-digital converters in the computer interface described by Greenwald (1972). Sample 1 delay (N4) controls the period from the start of the transmitter pulse to the first sample, and number of samples 1 (N5) determines how many sequential samples are taken. If the double-pulse option is being used, sample 2 (N7) and number of samples 2 (N8) are set as described in the operation section. The sample synch input is used to drive the data sampling control section from a recorded synch pulse when tape-recorded data are being analyzed on play-back. The sample output controls the digitizer, and the sample interrupt provides a means of stopping the sample sequence by an external device. The double sample jumper terminals must be connected for double-pulse operation.

All of the cards shown in Figure 27 that are controlled by front panel switches (N1 through N9) are identical N+1 frequency dividers. A schematic of the basic card is shown in Figure 28. This card can be triggered either from the clock or the external synch. Pin 1 of the 7408 is connected to the clock in cards N1, N3, and N9, and the output of these cards is a variable pulse rate for clocking purposes. Pin 1 (of the 7408) is connected to the external synch in cards N2, N4, N5, N6, N7, and N8 to provide an output delayed from the synch pulse by a time selected by the thumb-wheel switch. A timing diagram for this card is shown in Figure 29. This card will operate very reliably at clock frequencies up to 5 MHz.

The clock section shown in Figure 27 uses two basic divider cards plus a circuit card with a crystal oscillator. This section provides two variable clocks (N1 and N2) with frequencies determined by thumbwheel switches and three fixed frequency clocks (30-MHz,15-MHz,and 3-MHz). Figure 30 shows the schematic of the oscillator card. The 30-MHz crystal is connected to a divide-by-two network to give a 15-MHz output and also to a divide-by-ten network to provide a 3-MHz output. The 3-MHz signal is used as the clock input for the two variable clocks. Clock 1 (N9) is not used in this system, but provides a variable clock if needed. Clock 2 (N1) provides the time base for the system synchronizer.

The transmit/receive section shown in Figure 27 uses three basic divider cards plus the TX/TR output card. The circuit of the TX/TR card is shown in Figure 31. The transistors are used to convert the 0 to +5 volt logic signal to a -15 to +5 volt signal that drives the diodes in the diode switch and the TR switch.

The final section of the system synchronizer shown in Figure 27 is the data sampling section. The analog-to-digital converters (ADC's) in the computer interface are driven by this section. The sampling pulses reset the ADC's at the +5 volt or "1" level and digitization starts when the signal returns to the low or "0" level. The sampling section can be used either for on-line or playback data analysis. In the on-line mode, the sampling section operates synchronously with the transmitter. In the playback mode, the tape-recorded synch pulse is fed into the sample synch input. As shown in the sample input/output card schematic in Figure 32, the sample synch signal from the tape is amplified to the correct level to drive N4 (and N7 in the double-pulse mode). The amplification can be adjusted by a front panel control.

4.4 Synchronizer operation and timing

The synchronizer is normally connected in the Doppler radar system as shown in Figure 1. The system's operating parameters such as pulse length, pulse repetition frequency, sample 1 delay, and number of samples 1 are all set on the appropriate front panel switches of the system synchronizer. These parameters can be adjusted over a very wide range to accomodate any experimental configuration. The following two paragraphs provide examples for operating the system synchronizer in both single-pulse and double-pulse modes.

The timing diagram for single-pulse operation is shown in Figure 33. Note that the clock 2 period T is (2/3)(N1+1) microseconds. The pulse width is equal to N2 times T (in this example, N2=1). The interpulse period (IPP) equals (N3+1) times T (in this example N3=21). The TR drive pulse turns the TR switch on for one clock 2 period (T) before the transmitter is excited, and

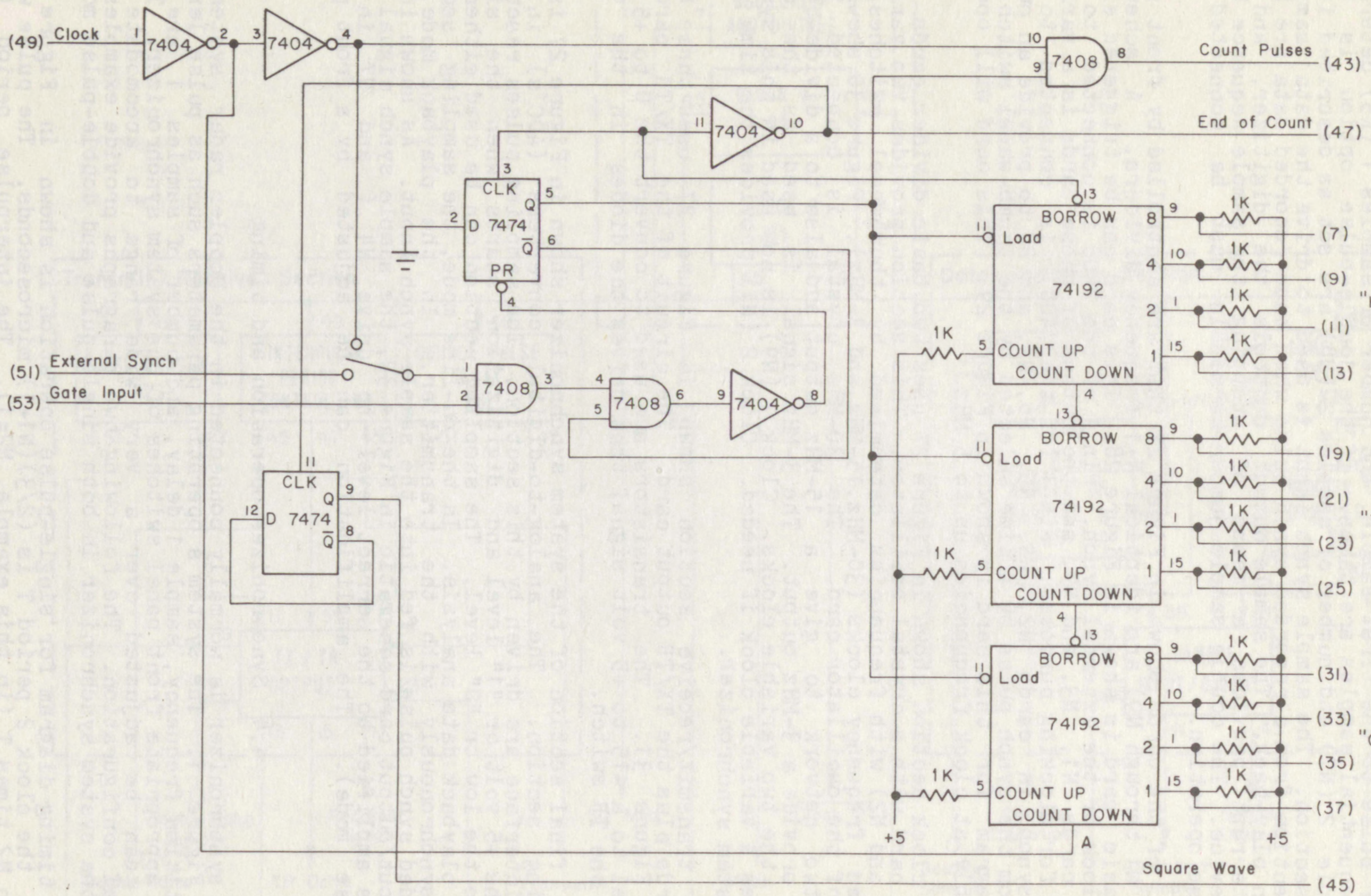

Figure 28. Schematic diagram of the basic circuit card.

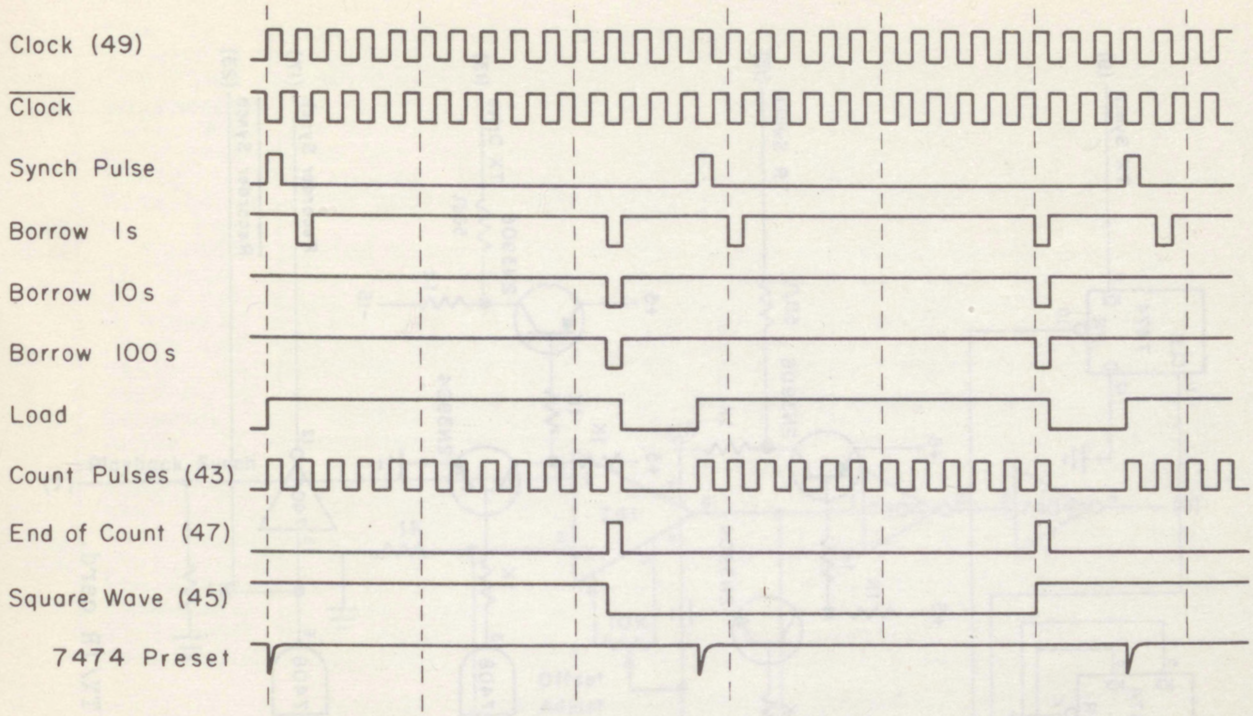

Figure 29. Timing diagram of the basic card.

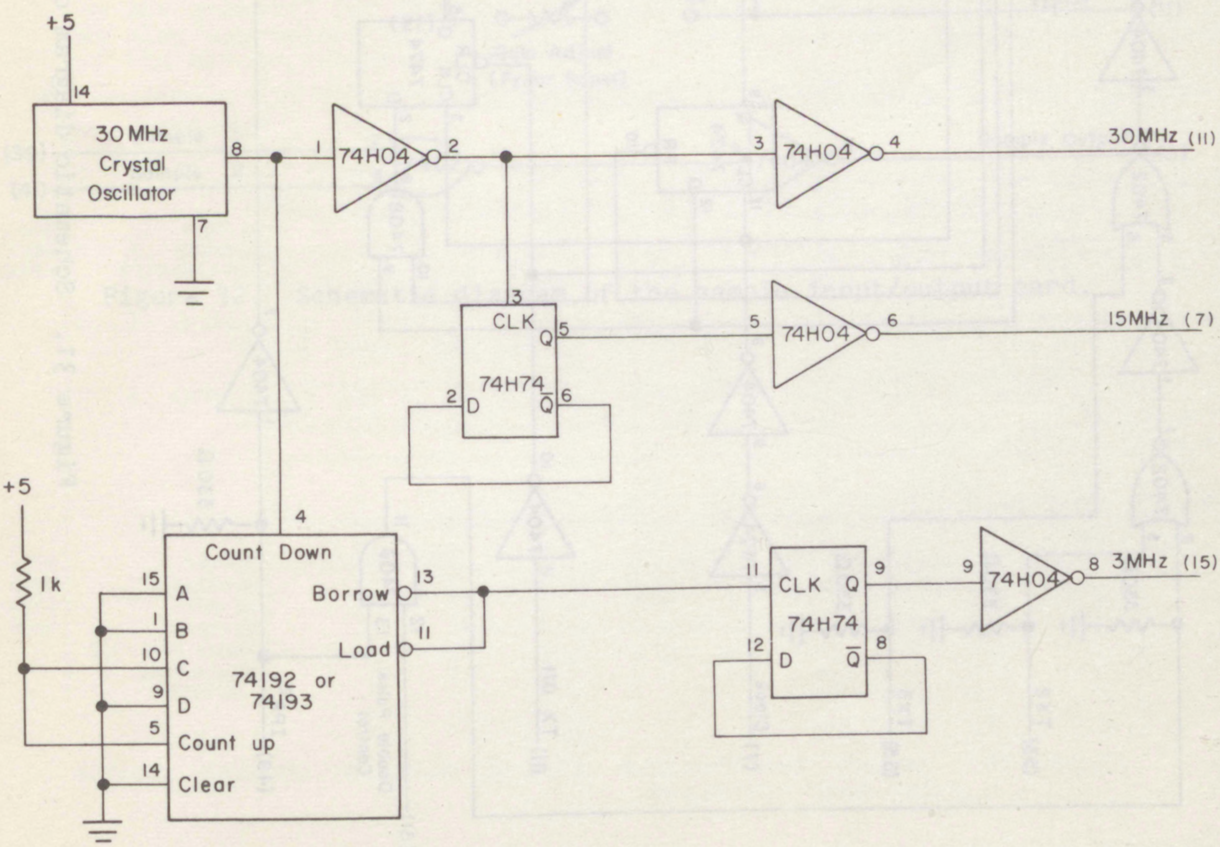

Figure 30. Schematic diagram of the oscillator card.

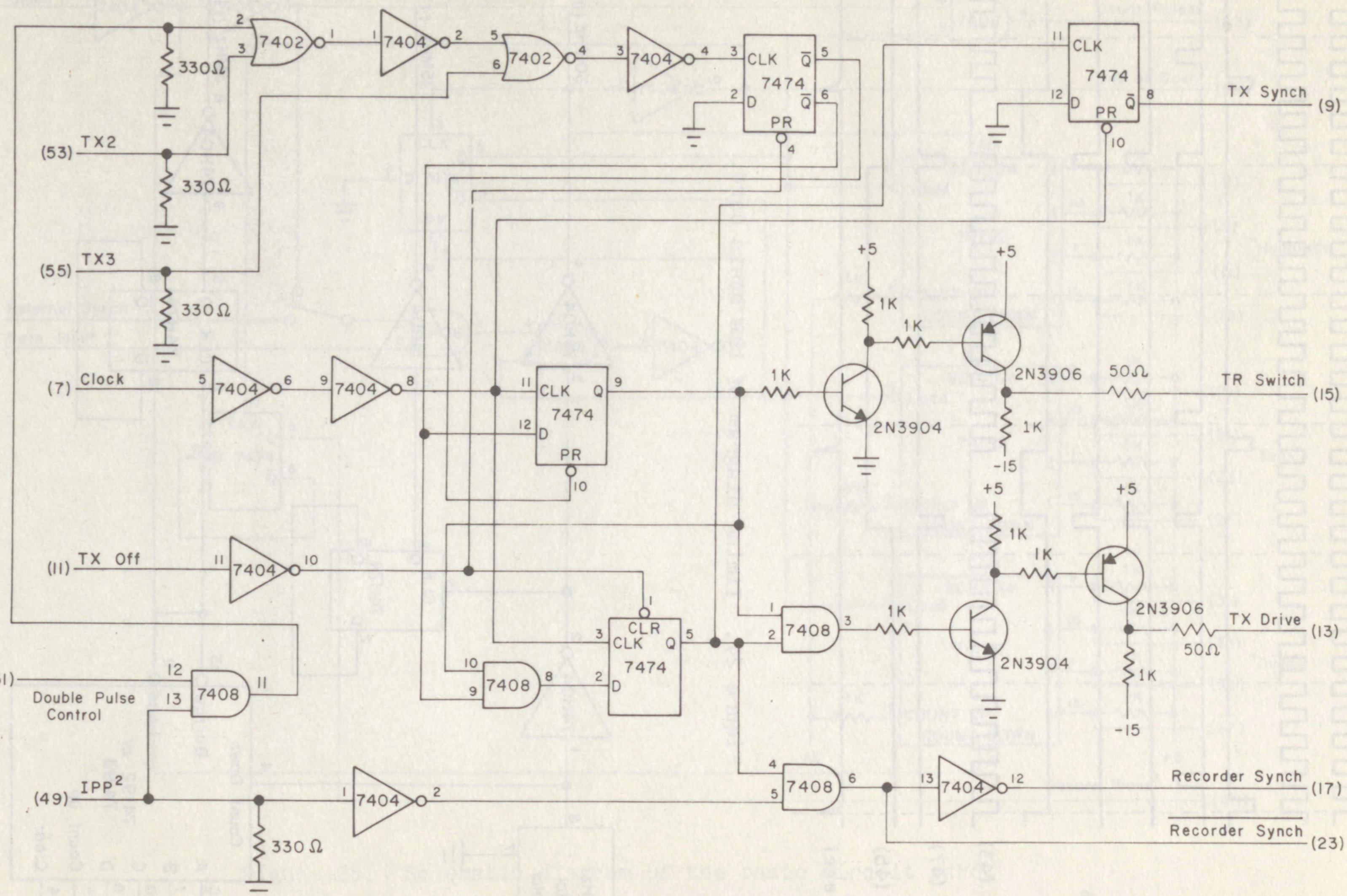

Figure 31. Schematic diagram of the TX/TR card.

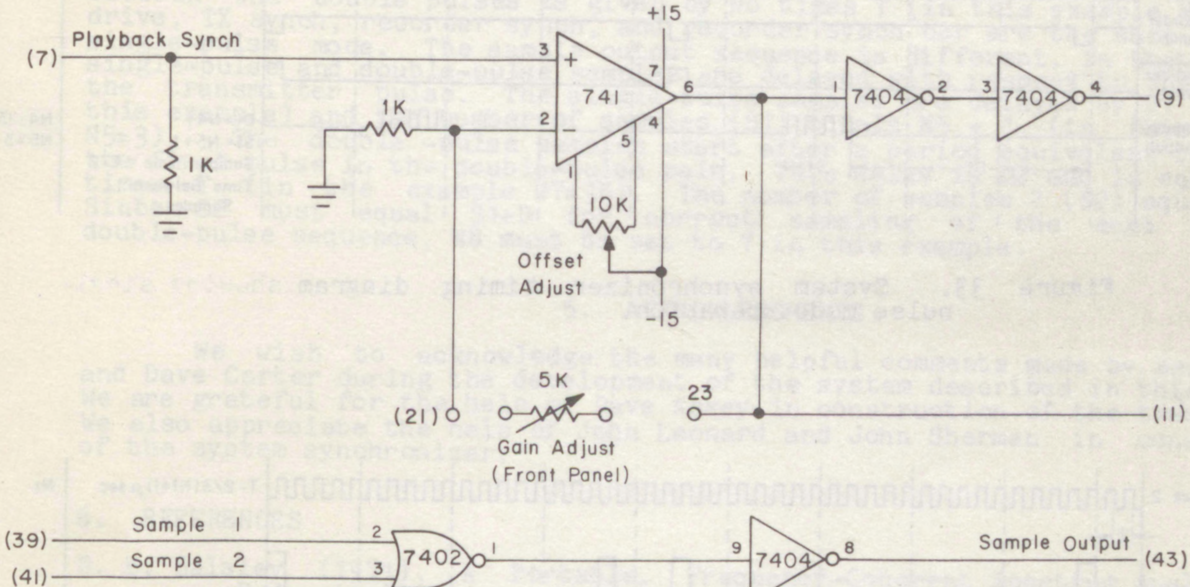

Figure 32. Schematic diagram of the sample input/output card.

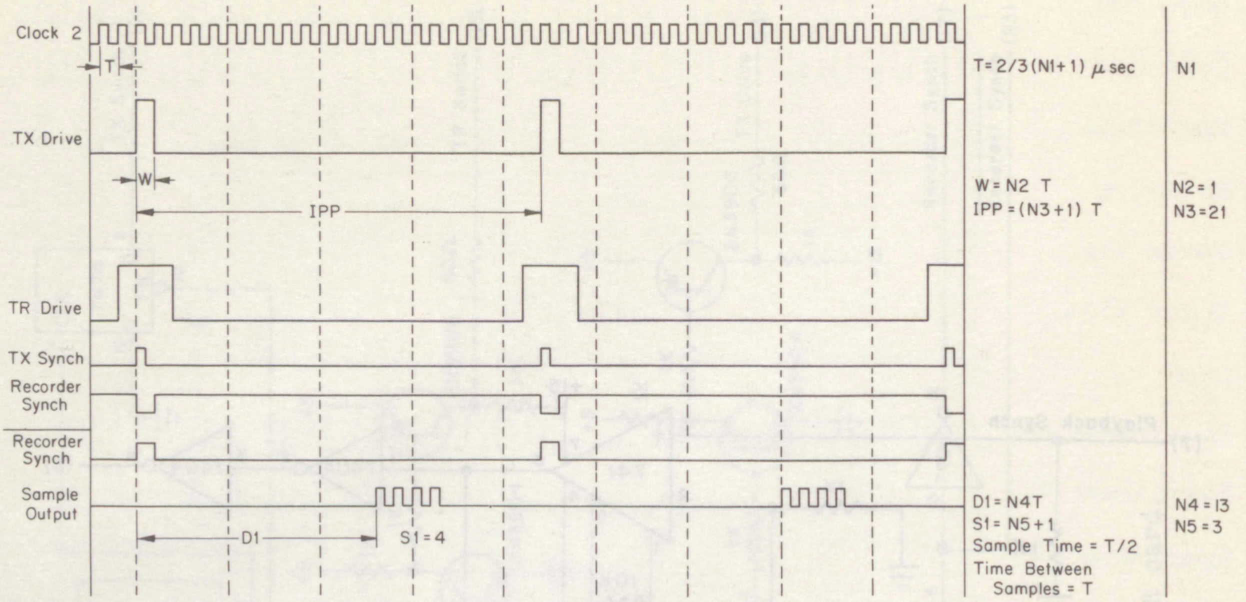

Figure 33. System synchronizer timing diagram showing single pulse mode operation.

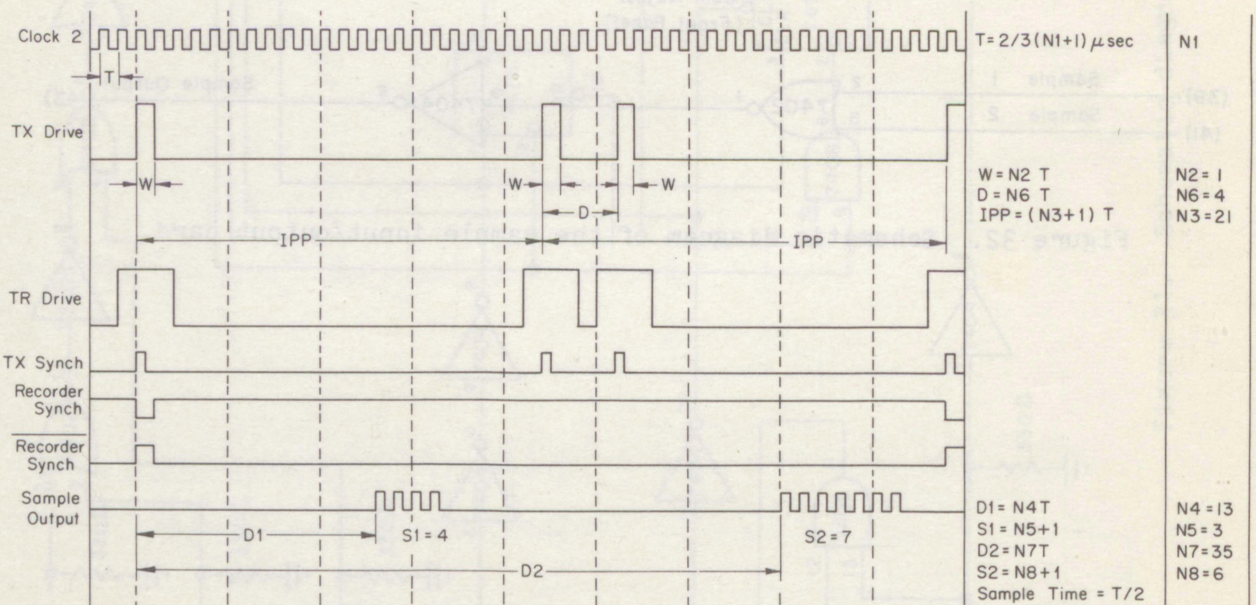

Figure 34. System synchronizer timing diagram showing double pulse mode operation.

the TR switch stays in the transmit mode for one clock 2 period after the transmitter excitation is removed. The TX synch pulse can be used to trigger the display scope sweep. Recorder synch and recorder synch bar provide timing pulses for the analog tape recorder. These recorded pulses correspond to the time when the transmitter is excited. The sample output starts at a delay D1 with respect to the transmitter pulse. D1 equals N4 times T. In this example N4=13. The number of samples (S1) equals N5+1. In this example N5=3. The time between the multiple samples is T.

The timing diagram for double-pulse operation is shown in Figure 34. In this mode, with both front panel jumpers in place, the transmitter sends out alternating single-pulse and double-pulse sequences as described by Greenwald and Ecklund (1975). The single pulse provides echo amplitude versus range information, and the double-pulse sequence provides mean Doppler versus range information. As in the single-pulse mode, N1 controls the clock 2 period, N2 controls the pulse width and N3 the interpulse period. The spacing between the double pulses is given by N6 times T (in this example N6=4). TR drive, TX synch, recorder synch, and recorder synch bar are the same as in the single-pulse mode. The sample output sequence is different, in that both the single-pulse and double-pulse samples are delayed with respect to the start of the transmitter pulse. The single-pulse samples are delayed by D1 (N4=13 in this example) and the number of samples (S1) equals N5 + 1 (in this example N5=3). The double -pulse samples start after a period equivalent to D1 from the first pulse in the double-pulse pair. This delay is D2 and is equal to N7 times T (in the example N7=35). The number of samples 2 (S2) equals N8+1. Since S2 must equal S1+D for correct sampling of the echo from the double-pulse sequence, N8 must be set to 7 in this example.

5. ACKNOWLEDGMENTS

We wish to acknowledge the many helpful comments made by Ben Balsley and Dave Carter during the development of the system described in this report. We are grateful for the help of Dave Askey in construction of the transmitter. We also appreciate the help of John Leonard and John Sherman in construction of the system synchronizer.

6. REFERENCES

B. B. Balsley (1971), A Portable, Frequency-Coherent Spectrum Analyzer for Radar Applications, NOAA Tech. Rept. ERL 204-AL 5.

B. B. Balsley and W. L. Ecklund (1972), A Portable Coaxial Collinear Antenna, IEEE Trans. Ant. Prop., AP-20: 513-516.

R. A. Greenwald (1972), Doppler Spectrum Analysis Using a Minicomputer, NOAA Tech. Rept. ERL 241-AL 7.

R. A. Greenwald and W. L. Ecklund (1975), A New Look at Radar Auroral Motions, submitted to JGR.

☆U.S. GOVERNMENT PRINTING OFFICE: 1976—677-347 / 1258 REGION NO.8

ENVIRONMENTAL RESEARCH LABORATORIES

The mission of the Environmental Reasearch Laboratories is to study the oceans, inland waters, the lower and upper atmosphere, the space environment, and the earth, in search of the understanding needed to provide more useful services in improving man's prospects for survival as influenced by the physical environment. Laboratories contributing to these studies are:

Atlantic Oceanographic and Meteorological Laboratories (AOML): Geology and geophysics of ocean basins and borders, oceanic processes, sea-air interactions and remote sensing of ocean processes and characteristics (Miami, Florida).

Pacific Marine Environmental Laboratory (PMEL): Environmental processes with emphasis on monitoring and predicting the effects of man's activities on estuarine, coastal, and near-shore marine processes (Seattle, Washington).

Great Lakes Environmental Research Laboratory (GLERL): Physical, chemical, and biological, limnology, lake-air interactions, lake hydrology, lake level forecasting, and lake ice studies (Ann Arbor, Michigan).

Atmospheric Physics and Chemistry Laboratory (APCL): Processes of cloud and preciptation physics; chemical composition and nucleating substances in the lower atmosphere; and laboratory and field experiments toward developing feasible methods of weather modification.

Air Resources Laboratories (ARL): Diffusion, transport, and dissipation of atmospheric contaminants; development of methods for prediction and control of atmospheric pollution; geophysical monitoring for climatic change (Silver Spring, Maryland).

Geophysical Fluid Dynamics Laboratory (GFDL): Dynamics and physics of geophysical fluid systems; development of a theoretical basis, through mathematical modeling and computer simulation, for the behavior and properties of the atmosphere and the oceans (Princeton, New Jersey).

National Severe Storms Laboratory (NSSL): Tornadoes, squall lines, thunderstorms, and other severe local convective phenomena directed toward improved methods of prediction and detection (Norman, Oklahoma).

Space Environment Laboratory (SEL): Solar-terrestrial physics, service and technique development in the areas of environmental monitoring and forecasting.

Aeronomy Laboratory (AL): Theoretical, laboratory, rocket, and satellite studies of the physical and chemical processes controlling the ionosphere and exosphere of the earth and other planets, and of the dynamics of their interactions with high-altitude meteorology.

Wave Propagation Laboratory (WPL): Development of new methods for remote sensing of the geophysical environment with special emphasis on optical, microwave and acoustic sensing systems.

Marine EcoSystem Analysis Program Office (MESA): Plans and directs interdisciplinary analyses of the physical, chemical, geological, and biological characteristics of selected coastal regions to assess the potential effects of ocean dumping, municipal and industrial waste discharges, oil pollution, or other activity which may have environmental impact.

Weather Modification Program Office (WMPO): Plans and directs ERL weather modification research activities in precipitation enhancement and severe storms mitigation and operates ERL's research aircraft.

NATIONAL OCEANIC AND ATMOSPHERIC ADMINISTRATION
BOULDER, COLORADO 80302